(Submitted to Earthquake Spectra in April, 2001.)

Structure-Specific Scalar Intensity Measures for Near-Source and Ordinary Earthquake Ground Motions

Nicolas Luco and C. Allin Cornell, M.EERI

Introduced in this paper are several scalar ground motion intensity measures (*IM*'s) that are each intended to be used in a performance assessment of a structure at a site susceptible to near-source and/or ordinary ground motions. A comparison of such *IM*'s is facilitated by defining the "efficiency" and "sufficiency" of an *IM*, which are both criteria that can be quantified via (a) nonlinear dynamic analysis of the structure under a suite of earthquake records, and (b) linear regression analysis. The efficiency and sufficiency of each of the alternative *IM*'s are demonstrated for the drift response of three different buildings of moderate-to-long period subjected to suites of ordinary and of near-source earthquake records. One of the alternative *IM*'s, in particular, is found to be relatively efficient and sufficient for both the near-source and the ordinary earthquake records, as well as for the range of buildings.

INTRODUCTION

At the core of recent performance-based seismic guidelines (FEMA 350-353 2000, Younan et al. 2001) is a scheme for assessing the mean annual frequency (or annual probability) of exceeding a specified limit state (e.g., the collapse limit state) for a given structure at a designated site. The Pacific Earthquake Engineering Research (PEER) center has also recently adopted the scheme as a "foundation on which performance assessment can be based" (http://peer.berkeley.edu/news/2000spring/performance.html). As expressed mathematically in Equation 1, the scheme "de-convolves" the assessment by introducing two intermediate variables: (a) a structural demand measure, *DM*, such as drift response, and (b) a ground motion intensity measure, *IM*, such as peak ground acceleration or spectral acceleration.

$$\lambda[LS] = \iint_{DM,\,IM} G[LS \mid DM]\,|\,\mathrm{d}G[DM \mid IM]\,|\,|\,\mathrm{d}\lambda[IM]\,|\,, \tag{1}$$

The mean annual frequency (MAF for short) of exceeding the limit state *LS*, denoted $\lambda[LS]$, can be used to make decisions about, for example, the adequacy of a design or the need to retrofit. In Equation 1, $G[LS|DM]$ denotes the probability of exceeding *LS* given (i.e., conditioned on knowing) the value of *DM*; typically, *LS* is defined indirectly by a (deterministic or random-valued) capacity with the same units as *DM*, in which case $G[LS|DM]$ is simply the probability that this capacity is less than the value of *DM*. The term $G[DM|IM]$ denotes the probability of exceeding each value of *DM* given the value of *IM*; it is

Dept. of Civil and Environmental Engineering, Stanford University, Stanford, CA 94305-4020

normally estimated using the results of nonlinear dynamic structural analysis (NDA for short) under a suite of earthquake ground motion records (Shome and Cornell 1999, Collins et al. 1995, Song and Ellingwood 1999). Lastly, $\lambda[IM]$ denotes the MAF of exceeding each value of *IM*, which is simply the ground motion hazard; $\lambda[IM]$ is typically computed via Probabilistic Seismic Hazard Analysis (PSHA) (Cornell 1968).

The ground motion intensity measure *IM* serves as a link between seismic hazard curves provided by seismologists (i.e., $\lambda[IM]$) and structural analysis conducted by engineers (to estimate $G[DM|IM]$). Beyond convention or convenience, the selection of an appropriate *IM* to be employed in Equation 1 for $\lambda[LS]$ is driven by the "efficiency" and the "sufficiency" of the *IM*. An efficient *IM* is defined simply (from the perspective of a structural engineer) as one that results in a relatively small variability of *DM* given *IM*, thereby reducing the number of NDA's and earthquake records necessary to estimate $G[DM|IM]$ with adequate precision (Shome and Cornell 1999). A sufficient *IM*, on the other hand, is defined here as one that renders *DM* conditionally independent, given *IM*, of earthquake magnitude (*M*) and source-to-site distance (*R*). As explained further in Appendix I, a sufficient *IM* is desirable because it ensures an accurate estimate of $G[DM|IM]$ and thereby an accurate estimate of $\lambda[LS]$ by Equation 1.

Based on its efficiency and sufficiency alone, note that the ultimate *IM* is actually *DM* itself. Of course, directly computing $\lambda[DM]$ via PSHA (in place of $\lambda[IM]$ in Equation 1 for $\lambda[LS]$) would require either a structure-specific attenuation relationship for *DM* or extensive ground motion simulation (Collins et al. 1995). In turn, both would call for NDA of the given structure under hundreds of ground motions from an array of *M*'s and *R*'s, which is impractical. This extreme alternative for *IM* emphasizes the need to bear in mind the computability of $\lambda[IM]$ in addition to the efficiency and the sufficiency of *IM* in selecting an appropriate intensity measure.

RECENT STUDIES

In applying the scheme for estimating $\lambda[LS]$ expressed by Equation 1, *IM* is conventionally (FEMA 350-353, Younan et al. 2001) taken to be the spectral acceleration at (or near) the fundamental period of the given structure (with a damping ratio of 5%), denoted here as $S_a(T_1)$. In part, this *IM* choice is driven by convenience, as seismic hazard curves in terms of $S_a(T_1)$ are either readily available (e.g., from the U.S. Geological Survey at http:/geohazards.cr.usgs.gov/eq/) or commonly computed. Moreover, several studies (e.g., Shome et al. 1998) have demonstrated (e.g., for drift response *DM*'s) that $S_a(T_1)$ is more "efficient" than peak ground acceleration (PGA), for example, presumably because $S_a(T_1)$ is period-specific. Nonetheless, recent studies have also demonstrated that $S_a(T_1)$ may not be particularly efficient, nor "sufficient," for some structures (e.g., tall, long period buildings) (Shome and Cornell 1999) or for near-source ground motions.

For tall, long period buildings, the higher modes typically contribute significantly to the seismic response (at least in the elastic range). Thus, as one might expect, $S_a(T_1)$ has been observed to be less efficient (i.e., the variability of *DM* given $S_a(T_1)$ is larger) for tall, long period buildings than it is for a shorter building whose response is dominated by the fundamental mode (Shome and Cornell 1999, Cornell and Luco 1999). Moreover, for tall, long period buildings $S_a(T_1)$ has been observed to be rather insufficient as well (i.e., given $S_a(T_1)$, *DM* still depends on *M*). Like the observed inefficiency, this insufficiency is presumably due to the fact that $S_a(T_1)$ does not reflect important higher-mode spectral

accelerations (i.e., spectral shape), which are dependent on M (Abrahamson and Silva 1997). Note, in addition, that for soft-soil or near-source ground motions with a predominant period near (for example) the second-mode period of the structure (i.e., T_2), the intensity measure $S_a(T_1)$ may prove particularly inefficient and insufficient. In order to gain efficiency and sufficiency when higher modes of response are important, Shome and Cornell (1999) and Bazzuro (1998) have considered a vector *IM* comprised of $S_a(T_1)$ and the ratio $S_a(T_2)/S_a(T_1)$, as well as a scalar *IM* that combines $S_a(T_1)$ and $S_a(T_2)$.

Under near-source ground motions, several studies (Baez and Miranda 2000, Bozorgnia and Mahin 1998, Alavi and Krawinkler 2000) have demonstrated that inelastic spectral displacements can be significantly larger than their elastic counterparts, even at periods for which the (predominantly non-near-source ground motion based) "equal displacements rule" (Veletsos and Newmark 1960) is expected to apply. At least for an inelastic single-degree-of-freedom (SDOF) structure of moderate period, this implies that $S_a(T_1)$ may not be as efficient for near-source ground motions as it is for "ordinary" (i.e., non-near-source) ground motions, which tend to uphold the equal displacements rule. The difference between inelastic and elastic spectral displacements under near-source earthquake records depends roughly on the predominant period of the ground motion (Alavi and Krawinkler 2000). To the extent that this predominant period depends on M (Somerville 1998), $S_a(T_1)$ may also be insufficient for near-source ground motions. Furthermore, $S_a(T_1)$ may be insufficient inasmuch as R is a proxy for near-source ground motions. For nonlinear multi-degree-of-freedom (MDOF) structures, a few studies (Alavi and Krawinkler 2000, Mehanny 1999) have demonstrated the inefficiency of $S_a(T_1)$ for near-source ground motions. In an attempt to gain efficiency for near-source ground motions, Deierlein et al. (i.e., Mehanny 1999, Cordova et al. 2001) have considered a scalar *IM* that combines $S_a(T_1)$ and $S_a(cT_1)$, where $c>1$ in order to reflect "softening" of an inelastic structure.

OBJECTIVE

This paper summarizes the authors' search, beginning with $S_a(T_1)$, for a scalar *IM* that is both "efficient" and "sufficient" with respect to drift response for buildings of moderate-to-long period subjected to "ordinary" or near-source earthquake ground motions. Keeping in mind the computability of the ground motion hazard $\lambda[IM]$, the space of possible *IM*'s is intentionally limited to measures that can be computed from only (a) modal vibration properties of the model structure (e.g., T_1 and T_2), (b) a nonlinear static-pushover (NSP for short) curve for the model structure, and (c) elastic or inelastic spectral displacements for the ground motion. Note that these are routinely attainable pieces of information about the structure and the ground motion. The *DM*'s investigated are limited to peak (over time) drift responses, and in this paper only results for maximum (over the height of a building) peak story drift angle (i.e., inter-story drift divided by story height), denoted $\theta_{\max}$, are presented. Corroborative results for individual peak story drift angles, as well as peak roof drift angles and average peak story drift angles, are presented in the first author's Ph.D. dissertation (Luco 2001).

DESCRIPTION OF *IM*'S, BUILDINGS, & EARTHQUAKE RECORDS

In this paper, the "efficiency" and "sufficiency" with respect to $\theta_{\max}$ of each of the six alternative *IM*'s introduced here are assessed for each of three different building models subjected to a suite of "ordinary" and a suite of near-source earthquake records. The details of and rationales for the alternative *IM*'s are explained here, but the ramifications in terms of

finding the ground motion hazard $\lambda[IM]$ for each *IM* are discussed below. The building models and suites of earthquake records are also described here.

EARTHQUAKE GROUND MOTION INTENSITY MEASURES (*IM*'S)

All of the *IM*'s considered in this paper can be thought of as (multiplicative) modifications of $S_a(T_1)$, which serves as a basis for comparison. Motivated by the shortcomings of $S_a(T_1)$ reviewed above, most of the modifications are intended to reflect the contributions of higher modes or the effects of inelasticity. Whereas the period-specific $S_a(T_1)$ requires only an estimate of T_1 (usually from an eigenvalue analysis) and an SDOF earthquake time-history analysis, the *IM*'s detailed here are more structure-specific in that they also make use of a roof-drift versus base-shear NSP curve, higher-mode periods, modal damping ratios, and modal participation factors. Also note that the alternative *IM*'s are expressed here specifically in relation to θ_{max}; similar expressions with respect to peak story drift angles, peak roof drift angles, and average peak story drift angles are provided in (Luco 2001).

Inspired by modal analysis, the first ground motion intensity measure IM_{1E} is simply the first-mode elastic estimate of θ_{max}. Like $S_a(T_1)$, IM_{1E} involves only the first-mode vibration properties of the model structure and an SDOF time-history analysis for the ground motion. As expressed in Equation 2, IM_{1E} is the product of $|PF_1^{[1]}|$, the model structure's first-mode participation factor for θ_{max} (refer to Appendix II for details), and $S_d(T_1,\zeta_1)$, the first-mode spectral displacement for the ground motion. Note that the damping ratio ζ_1 for the first mode is not necessarily equal to 5%, as assumed for $S_a(T_1)$.

$$IM_{1E} \quad = \quad |PF_1^{[1]}| \, S_d(T_1,\zeta_1) \qquad \tilde{\propto} \quad S_a(T_1), \tag{2}$$

Under the assumptions that (a) spectral displacement and acceleration are related by the period of interest (i.e., $S_d=(T/2\pi)^2 \cdot S_a$), and (b) spectral accelerations for different damping ratios but the same period are proportional (a rough approximation), IM_{1E} is proportional to $S_a(T_1)$ and the two are equivalent in terms of efficiency and sufficiency. In what follows, IM_{1E} replaces $S_a(T_1)$ as the basis for comparison.

Given that the *DM* of interest (here) is nonlinear structural drift, it is logical to consider an inelastic spectral displacement as the intensity measure, particularly for near-source ground motions under which the effects of inelasticity on spectral displacements can be substantial (as cited above). As expressed in Equation 3, IM_{1I} is the inelastic spectral displacement $S_d^I(T_1,\zeta_1,d_y)$ multiplied by the same first-mode participation factor for θ_{max}, $|PF_1^{[1]}|$, that is applied in Equation 2 for IM_{1E}. Also shown in Equation 2, IM_{1I} can be written as IM_{1E} multiplied by the ratio of $S_d^I(T_1,\zeta_1,d_y)$ to the corresponding elastic spectral displacement $S_d(T_1,\zeta_1)$.

$$IM_{1I} \quad = \quad |PF_1^{[1]}| \, S_d^I(T_1,\zeta_1,d_y) \qquad = \quad \frac{S_d^I(T_1,\zeta_1,d_y)}{S_d(T_1,\zeta_1)} \; IM_{1E}, \tag{3}$$

In this paper, $S_d^I(T_1,\zeta_1,d_y)$ is the spectral displacement of an elastic-perfectly-plastic (EPP) oscillator with period T_1, damping ratio ζ_1, and yield-displacement d_y; as explained in Appendix III, d_y can be determined via a NSP of the model structure of interest. As noted in the conclusions of this paper, other backbone curves for the inelastic oscillator are considered in (Luco 2001).

Whereas IM_{1E} and IM_{1I} reflect only the fundamental mode of structural response, the ground motion intensity measure $IM_{1E\&2E}$ is the estimate of $\theta_{\max}$ using the first two modes and the square-root-of-sum-of-squares (SRSS) rule of modal combination, as expressed in Equation 4. At least in the event of elastic response, $IM_{1E\&2E}$ is an improved estimate of $\theta_{\max}$ if higher modes contribute significantly to the structural response (e.g., for tall, long period structures).

$$\begin{aligned} IM_{1E\&2E} &= \sqrt{[PF_1^{[2]} S_d(T_1,\zeta_1)]^2 + [PF_2^{[2]} S_d(T_2,\zeta_2)]^2} \\ &= \sqrt{1+R_{2E/1E}^2}\left|\frac{PF_1^{[2]}}{PF_1^{[1]}}\right| IM_{1E} \quad \text{where } R_{2E/1E} = \frac{PF_2^{[2]} S_d(T_2,\zeta_2)}{PF_1^{[2]} S_d(T_1,\zeta_1)} \end{aligned}, \qquad (4)$$

Also noted in Equation 4, $IM_{1E\&2E}$ can be written as IM_{1E} multiplied by two modification factors: the first (i.e., the square root term) accounts for the (elastic) contribution of the second mode to $\theta_{\max}$ and thereby reflects the relevant spectral shape, whereas the second (i.e., the absolute value term) adjusts for the fact that the first-mode estimate and the first-two-modes estimate of $\theta_{\max}$ may correspond to different stories. Note that $PF_1{}^{[2]}$ denotes the first-mode participation factor for the story corresponding to the first-two-mode SRSS estimate of $\theta_{\max}$; similarly, $PF_1{}^{[1]}$ is the first-mode participation factor for the story corresponding to the first-mode (only) estimate of $\theta_{\max}$. Refer to Appendix II for more details.

In an attempt to reflect both the contribution of the second mode (in addition to the first) and the effects of nonlinearity, the ground motion intensity measure $IM_{1I\&2E}$ is considered. As expressed in Equation 5, $IM_{1I\&2E}$ is equal to $IM_{1E\&2E}$ multiplied by the ratio of $S_d^I(T_1,\zeta_1,d_y)$ to $S_d(T_1,\zeta_1)$ (i.e., the same ratio of inelastic to elastic spectral displacements that is applied for IM_{1I} in Equation 3). Also expressed in Equation 5 is the fact that $IM_{1I\&2E}$ can be found by substituting IM_{1I} for IM_{1E} in Equation 4 for $IM_{1E\&2E}$.

$$IM_{1I\&2E} = \frac{S_d^I(T_1,\zeta_1,d_y)}{S_d(T_1,\zeta_1)} IM_{1E\&2E} = \sqrt{1+R_{2E/1E}^2}\left|\frac{PF_1^{[2]}}{PF_1^{[1]}}\right| IM_{1I}, \qquad (5)$$

Note that, in effect, $IM_{1I\&2E}$ supposes a relationship between the ratio of nonlinear to elastic MDOF drift response (i.e., $\theta_{\max}/IM_{1E\&2E}$) and the ratio of $S_d^I(T_1,\zeta_1,d_y)$ to $S_d(T_1,\zeta_1)$.

To avoid inelastic SDOF time-history analysis, the inelastic spectral displacement required for IM_{1I} and $IM_{1I\&2E}$ (Equations 3 and 5, respectively) can be replaced by the spectral displacement of an "equivalent" elastic SDOF oscillator, denoted $S_d^{eq}(T_1,\zeta_1,d_y)$. Doing so for IM_{1I} results in the ground motion intensity measure IM_{1eq}, as expressed in Equation 6.

$$IM_{1eq} = |PF_1^{[1]}| S_d^{eq}(T_1,\zeta_1,d_y) = \frac{S_d^{eq}(T_1,\zeta_1,d_y)}{S_d(T_1,\zeta_1)} IM_{1E}, \qquad (6)$$

In this paper, the period and damping of the equivalent elastic oscillator are established using the empirical formulas developed by Iwan (1980). These formulas are functions of ductility, which is merely approximated here by $S_d(T_1,\zeta_1)/d_y$. Alternatively, the period and damping of the equivalent elastic oscillator could be established by a procedure resembling the Capacity Spectrum Method (Freeman et al. 1975), for example.

Another *IM* that attempts to capture the effects of inelasticity by considering the elastic spectrum at an "effective" period longer than T_1 (reflecting a reduction in stiffness) has been proposed by Deierlein et al. (i.e., Mehanny 1999, Cordova et al. 2001). As noted at the far right of Equation 7, the proposed *IM* is a function of both $S_a(T_1)$ and $S_a(cT_1)$, where $c>1$. By optimizing the efficiency of the proposed *IM* for a specific set of model structures and earthquake records, Cordova et al. (2001) have calibrated c and α to equal 2 and 1/2, respectively.

$$IM_{1eff} = \sqrt{\frac{S_d(2T_1,\zeta_1)}{2S_d(T_1,\zeta_1)}}\ IM_{1E} \quad \approx\approx \quad S_a(T_1)\left[\frac{S_a(cT_1)}{S_a(T_1)}\right]^{\alpha} \text{ where } c=2\,,\ \alpha=\frac{1}{2}, \quad (7)$$

As expressed in Equation 7, IM_{1eff} is (approximately) proportional to the ground motion intensity measure proposed by Deierlein et al., but is formulated here as a modification of IM_{1E} that involves only spectral displacements. Note that the factor of 2 introduced in front of $S_d(T_1,\zeta_1)$ renders the modification factor equal to one if spectral displacement increases proportionally with period (i.e., as it would in the "constant-velocity" realm of a spectrum).

It should be noted that the basic components of the scalar modifications of $S_a(T_1)$ that are introduced here (e.g., $S_d^I(T_1,\zeta_1,d_y)/S_d(T_1,\zeta_1)$ and $S_a(T_1)$ for IM_{1I}) could instead be considered as separate elements of a vector-valued *IM*. Employing a vector-valued *IM*, however, requires certain extensions to conventional PSHA (Bazzurro 1998). Moreover, the scalar *IM*'s considered here are easier to interpret, particularly because their units are the same as those for the *DM* of interest, namely radians for $\theta_{\max}$.

BUILDING MODELS

The structures considered in this study are the 3-story, 9-story, and 20-story steel moment-resisting frame (SMRF) buildings designed for Los Angeles conditions by consulting structural engineers as part of the SAC Steel Project (Phase II). The designs were carried out according to pre-Northridge earthquake practices (i.e., 1994 Uniform Building Code). Only the perimeter frames of each building are moment resisting; the interior frames are intended to support gravity loads only. Detailed descriptions of the SAC buildings can be found in (Gupta and Krawinkler 1999) and (Luco 2001).

Under the assumption of a rigid diaphragm, a two-dimensional centerline model of each of the three (relatively symmetric) buildings is created for nonlinear analysis using DRAIN-2DX (Prakash et al. 1993). Each analysis model accounts for both the perimeter MRF's and the interior gravity frames. The nonlinear analyses take into account P-Δ effects, ductile plastic hinging (with 3% strain hardening) at beam-ends, column-ends, and column-splices, and M-P interaction. Rather than modeling the shear connections (e.g., in the gravity frames) as "pins," they are each attributed stiffness and strength properties reasonably close to those observed in laboratory tests carried out by Liu and Astaneh-Asl (2000).

The periods and damping ratios for the first two modes of each of the three buildings models, as well as the yield displacement d_y associated with the first mode (as defined in Appendix III), are listed in Table 1. Along with the participation factors (described in detail in Appendix II), the information in Table 1 is used to calculate the *IM*'s introduced above. For convenience in calculating the *IM*'s, however, the damping ratios ζ_1 and ζ_2 are set equal to 0.02 for all three building models. Note that for brevity, the Los Angeles 3-, 9-, and 20-story building models are hereafter referred to as LA3, LA9, and LA20.

Table 1. First and second mode properties of the SMRF building models.

Building model	First mode			Second mode	
	T_1 (sec)	ζ_1	d_y (cm)	T_2 (sec)	ζ_2
LA3	0.98	0.020	12	0.30	0.016
LA9	2.23	0.020	33	0.82	0.011
LA20	3.96	0.021	41	1.35	0.012

EARTHQUAKE GROUND MOTION RECORDS

Both "ordinary" and near-source earthquake ground motion records are considered in this paper. The suite of "ordinary" earthquake records consists of ground motions with closest distances to the rupture surface (i.e., *R*) between 30 and 46 kilometers. The suite of near-source earthquake records, on the other hand, is restricted to ground motions with *R* less than 16 kilometers, motivated by the SEAOC Blue Book (1999). Furthermore, the near-source suite is restricted to "forward-directivity" earthquake records, whereas the ordinary suite excludes such earthquake records. Here a forward-directivity earthquake record is defined as one for which the rupture directivity modification factor for average $S_a(T)$, developed by Somerville et al. (1997a), is greater than one (at T = 1, 2, *and* 4 seconds, which are near the T_1's of the three building models considered). Because forward-directivity is generally manifested as a "pulse-like" ground motion perpendicular to the fault, the strike-normal component of each of the near-source earthquake records is considered. Likewise, in order to be consistent, the strike-normal components of the ordinary earthquake records are considered.

The ordinary and near-source suites of earthquake records are selected from the PEER Strong Motion Database (http://peer.berkeley.edu/smcat). In addition to the constraints based on *R* and forward-directivity, all of the earthquake records selected also satisfy the following criteria: (a) earthquake moment magnitude (i.e., *M*) greater than or equal to 6.0 (and less than or equal to 7.4), (b) recorded on "stiff soil" or "very dense soil and soft rock" (e.g., FEMA 273 (1997) site classes D or C, respectively), and (c) processed record with a maximum (between two horizontal components) high-pass filter corner-frequency less than or equal to 0.25 hertz. The 31 near-source earthquake records selected are from the Imperial Valley earthquake of 1979 (station codes H-BRA, H-ECC, H-EMO, H-E01, H-E04, H-E05, H-E06, H-E07, H-E08, H-E10, H-E11, H-EDA, H-WSM, H-PTS), the Superstition Hills earthquake of 1987 (station codes B-ICC, B-WSM, B-PTS), the Northridge earthquake of 1994 (station codes LOS, JEN, NWH, RRS, SPV, RO3, SCS, SCE, SYL, ARL, WPI, PAC, PKC), and the Loma Prieta earthquake of 1989 (station code WVC). It is interesting to note that not all of these near-source earthquake records are clearly "pulse-like" (a subjective description), even though they are (objectively) identified as "forward-directivity" ground motions with R<16km. The reader is referred to (Luco 2001) for time-history plots of the 31 near-source earthquake records, as well as the 59 earthquake records selected for the ordinary suite. Note that a 60th ordinary earthquake record (from the Coalinga earthquake of 1983, station code H-C04) that meets the above criteria is excluded for reasons discussed in (Luco 2001).

To augment the near-source suite, 6 additional "pulse-like" earthquake records from Somerville et al. (1997b, 1998) via Alavi and Krawinkler (2000) are also considered (refer to (Luco 2001) for a list). These supplemental ground motions were not originally recorded on "stiff soil" or "very dense soil and soft rock," but most of them were modified by Somerville et al. to reflect "stiff soil" conditions. Due to this difference, the results for the 6

supplemental pulse-like earthquake records are considered separately. Note that another 6 of the 15 pulse-like earthquake records considered by Alavi and Krawinkler are among the 31 in the near-source suite.

In order to investigate higher levels of nonlinear response, the near-source earthquake records considered are scaled as a suite (i.e., all earthquake records scaled by the same constant) by a factor of two. Correspondingly, the ordinary earthquake records are scaled as a suite by a factor of eight. This factor is chosen such that the 84th-percentile (i.e., "1-sigma level") elastic spectral displacements at the T_1's and ζ_1's of the three building models are approximately the same for the ordinary and near-source earthquake records.

APPROACH

As mentioned in the introduction, $G[DM|IM]$ in Equation 1 for $\lambda[LS]$ is normally estimated for a given structure using *DM* results from NDA under a suite of earthquake ground motions. Specifically, $G[DM|IM]$ can be estimated via a regression of the *DM* results on the corresponding values of *IM* (together with an assumed type of probability distribution for *DM* given *IM*) (Shome and Cornell 1999, Cornell and Luco 1999). In this case, the efficiency of *IM* is gauged by the degree of scatter about the regression (of *DM* on *IM*) fit, whereas the sufficiency of *IM* is gauged by the extent to which, after regressing on *IM*, the residual *DM* is statistically independent of *M* and *R*. In short, like $G[DM|IM]$, the efficiency and sufficiency of an *IM* can be quantified via regression analysis.

In this paper, a one-parameter log-log linear regression of $\theta_{\max}$ (the *DM*) on *IM* is utilized in assessing the efficiency and sufficiency of each alternative *IM*. The regression model is expressed in Equation 8, where a is the parameter (or coefficient) to be estimated and $\varepsilon|IM$ is the (random) error in $\theta_{\max}$ given *IM*.

$$\theta_{\max} = a \cdot IM \cdot (\varepsilon \mid IM) \quad \Leftrightarrow \quad \ln(\theta_{\max} / IM) = \ln(a) + \ln(\varepsilon \mid IM), \tag{8}$$

Note that a log-log scale is employed primarily because with it the variability of $\theta_{\max}$ given *IM* is observed (here and in (Shome and Cornell 1999), for example) to be roughly uniform over the range of *IM* values. In other words, it is anticipated that the standard deviation of $\ln(\varepsilon|IM)$, hereafter denoted simply as σ, will be approximately constant, which is an assumption of standard linear regression analysis (i.e., homoscedasticity). Furthermore, $\varepsilon|IM$ (or $\theta_{\max}$ given *IM*) is observed to be approximately lognormally distributed, so the log-log scale makes it possible to take advantage of normality assumptions (e.g., in quantifying the statistical significance of differences among estimates of a and of σ).

The one-parameter model expressed in Equation 8 is utilized instead of a standard two-parameter log-log linear regression model (which includes an exponent on *IM*) (Shome and Cornell 1999, Cornell and Luco 1999) for several reasons. In general, for drifts from 0% to 10% the one-parameter model is observed (e.g., in the results below) to be adequate for regressing $\theta_{\max}$ on each of the alternative *IM*'s investigated. That is, the nonlinear regression model employing an exponent on *IM* is generally not necessary, except for some cases in which the simple intensity measure IM_{1E} is employed. For these cases, the two-parameter model is also considered in (Luco 2001). In contrast to the two-parameter model, the one-parameter model is attractive in that the coefficient a can be interpreted as the bias of *IM* in estimating $\theta_{\max}$. Moreover, the one-parameter regression analysis amounts to merely calculating the "median" (strictly the geometric mean, or the exponential of the mean of the

natural logarithm) of the ratio θ_{max}/IM as the least-squares estimate of a, and the "dispersion" (strictly the standard deviation of the natural logarithm) of θ_{max}/IM in order to estimate σ.

As alluded to above, σ (i.e., the dispersion of θ_{max} given *IM*) serves as a measure of the efficiency of *IM* (regardless of the regression model). This is because, based on the simplest notions of statistics, σ is directly related to the number of earthquake records and NDA's, denoted n, that is necessary to estimate a with adequate precision (e.g., $\sigma_a \leq 0.10$), as expressed in Equation 9 (e.g., Benjamin and Cornell 1970). Note that σ_a is actually the standard deviation *of the regression estimate* of a, which could more formally be denoted as $\sigma_{\hat{a}}$.

$$n = (\sigma / \sigma_a)^2 , \tag{9}$$

According to Equation 9, if a particular choice of one *IM* over another reduces σ from, for example, 0.3 to 0.2, then n will be roughly halved, doubling the efficiency.

Using the one-parameter regression model expressed in Equation 8 also simplifies the procedure for quantifying the sufficiency of *IM*. Generally, *IM* can be regarded as sufficient if the coefficients on *M* and *R* estimated from a regression of θ_{max} on *IM*, *M*, and *R* are not statistically significant; for this paper, this condition is simplified (in an approximate way) by considering *M* and *R one at a time*. Beginning with the one-parameter model for the regression of θ_{max} on *IM*, a regression of θ_{max} on *IM* and *M* (or *R*) can be accomplished with a standard univariate linear regression (i.e., $y=\beta_0+\beta_1 x+\varepsilon$), as expressed in Equations 10a (or 10b). Similar to the notation used in Equation 8 above, *a'* and *c* are the regression parameters to be estimated and $\varepsilon|(IM,M)$ (or $\varepsilon|(IM,R)$) is the random error in θ_{max} given *IM* and *M* (or *R*). Note that the assumed log-linear dependencies on *M* and on ln(*R*) are consistent with the first order terms in standard attenuation relations (e.g., Abrahamson and Silva 1997).

$$\ln(\theta_{max} / IM) = \ln(a') + c \cdot M + \ln(\varepsilon \mid IM, M) , \tag{10a}$$

$$\ln(\theta_{max} / IM) = \ln(a') + c \cdot \ln(R) + \ln(\varepsilon \mid IM, R) , \tag{10b}$$

According to the one-parameter regression model expressed in Equation 8, $\ln(\theta_{max}/IM)$ is within a constant of $\ln(\varepsilon|IM)$, hence Equations 10a and 10b can be rewritten as Equations 11a and 11b, respectively.

$$\ln(\varepsilon \mid IM) = \ln(a'') + c \cdot M + \ln(\varepsilon \mid IM, M) , \tag{11a}$$

$$\ln(\varepsilon \mid IM) = \ln(a'') + c \cdot \ln(R) + \ln(\varepsilon \mid IM, R) , \tag{11b}$$

Equations 11a and 11b reveal that the coefficient c on *M* or ln(*R*) can conveniently be estimated via a standard linear regression of the observed values of $\ln(\varepsilon|IM)$ (i.e., the "residuals") on the corresponding values of *M* or ln(*R*). These equations are only valid, though, if the one-parameter model expressed in Equation 8 is adopted for regressing θ_{max} on *IM*.

The statistical significance of the regression estimate of the coefficient c on *M* or ln(*R*), and thereby the sufficiency of *IM*, can be quantified by the *p*–value for the c estimate (which is commonly reported by linear regression software). The *p*–value is defined as the probability of finding an estimate of c at least as large (in absolute value) as that observed if, in fact, the true value of c is 0 (e.g., Benjamin and Cornell 1970). Hence, a small *p*–value

(e.g., less than about 0.05) suggests that the estimated coefficient c on M or ln(R) is statistically significant, and therefore that IM is insufficient.

RESULTS

Using the regression analysis approach detailed in the previous section, here the efficiency and sufficiency (as well as the bias) of each of the *IM*'s investigated are quantified. First, pair-wise comparisons of the alternative *IM*'s are made for the most pertinent building model (i.e., LA3, LA9, or LA20) and suite(s) of earthquake records (i.e., "ordinary" and/or near-source). For the first few pair-wise IM comparisons, the regression of θ_{max} on IM (as expressed by Equation 8 above) is illustrated with a figure. The figure depicts the data and the regression fit, and lists the regression estimates for the coefficient a and for σ; the number of data points, n, is also listed. Although θ_{max} is the dependent variable in the regression of θ_{max} on IM, it is plotted as the abscissa, as per a traditional force (in this case IM) versus deformation (here θ_{max}) plot. Recall that a is a measure of the bias of the ground motion intensity measure IM in estimating θ_{max}, and σ is a measure of the efficiency of IM. The regression of the observed $\varepsilon|IM$ residuals on M or R (as expressed by Equation 11a or 11b above) that is conducted in order to measure the sufficiency of IM is also illustrated with a figure. Noted in the figure are the regression estimate of the coefficient c, the p–value for the estimate of c, and the regression estimate of the variability of $\varepsilon|(IM,M)$ or $\varepsilon|(IM,R)$ (also denoted simply as σ). Recall that a small p–value (e.g., less than about 0.05) suggests that the estimated coefficient c on M or R is statistically significant and hence that IM is insufficient. In all of the figures, each of the θ_{max} versus IM data points is plotted as the number (within a circle) of the story in which θ_{max} occurs. In addition to the pair-wise IM comparisons, the regression analysis results for the "primary" intensity measures IM_{1E}, IM_{1I}, $IM_{1E\&2E}$, and $IM_{1I\&2E}$ are summarized in a table for every combination of the three building models and two suites of earthquake records.

$IM_{1E\&2E}$ VS. IM_{1E} (FOR LA20 UNDER ORDINARY GROUND MOTIONS)

As cited above, recent studies have demonstrated that $S_a(T_1)$, or equivalently IM_{1E}, can be relatively inefficient and insufficient when considering tall, long period building models for which higher modes contribute significantly to the response (at least in the elastic range). This shortcoming of IM_{1E}, as well as the relative efficiency and sufficiency of $IM_{1E\&2E}$ (which accounts for the second mode), are demonstrated here with the LA20 building model subjected to the ordinary earthquake records. Note that 2 of the 59 ordinary earthquake records (which, recall, have been scaled up by a factor of 8) are excluded here because they cause "collapse" of the LA20 building model.

As described generically above, the regression of θ_{max} on IM_{1E} is illustrated in Figure 1. First note the broad range of θ_{max} values, from less than 0.01 radians (effectively elastic) to almost 0.07 radians, a story ductility of about 7. The estimated regression coefficient (a=1.59) indicates that IM_{1E} is biased low (i.e., on average, IM_{1E} under-estimates θ_{max}). In fact, IM_{1E} under-estimates θ_{max} for most of the ground motions, as evidenced by the data points in Figure 1 that lie below the one-to-one dashed line. At least in the elastic range, it is not surprising that IM_{1E} is biased low, for it does not take into account the contributions to θ_{max} from higher modes. Meanwhile, the comparatively large scatter about the regression fit in Figure 1 (quantified by σ=0.44) indicates that IM_{1E} is relatively inefficient as well. Recall that, according to Equation 9, σ=0.44 implies that at least 20 earthquake records must be

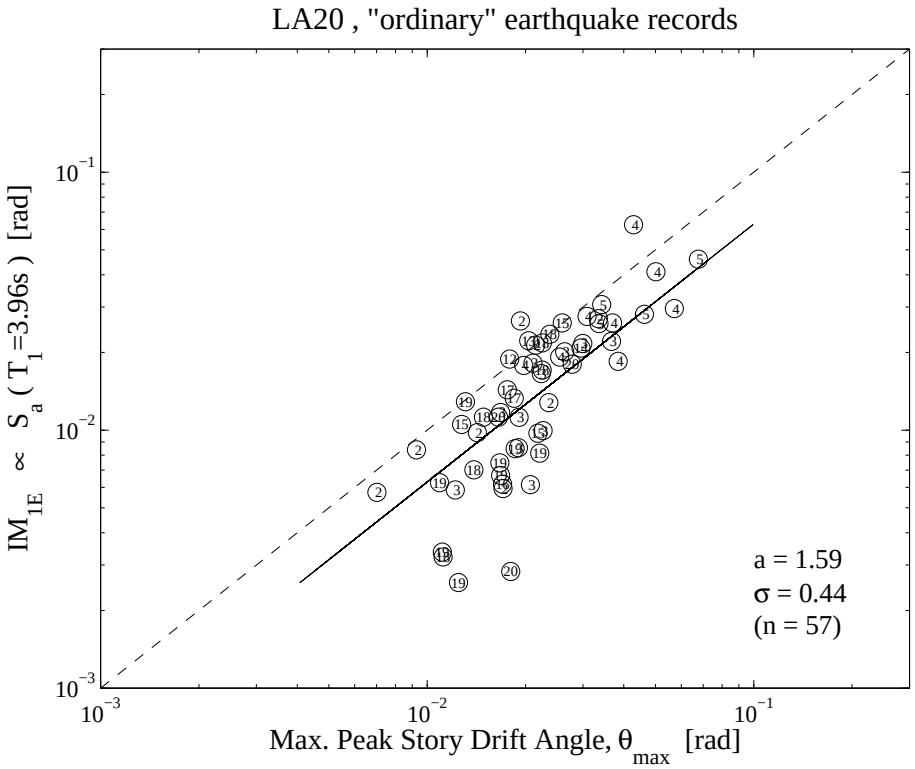

Figure 1. Regression of θ_{max} (from NDA) on ground motion intensity measure IM_{1E}, in order to quantify the bias (a) and efficiency (σ) of IM_{1E}.

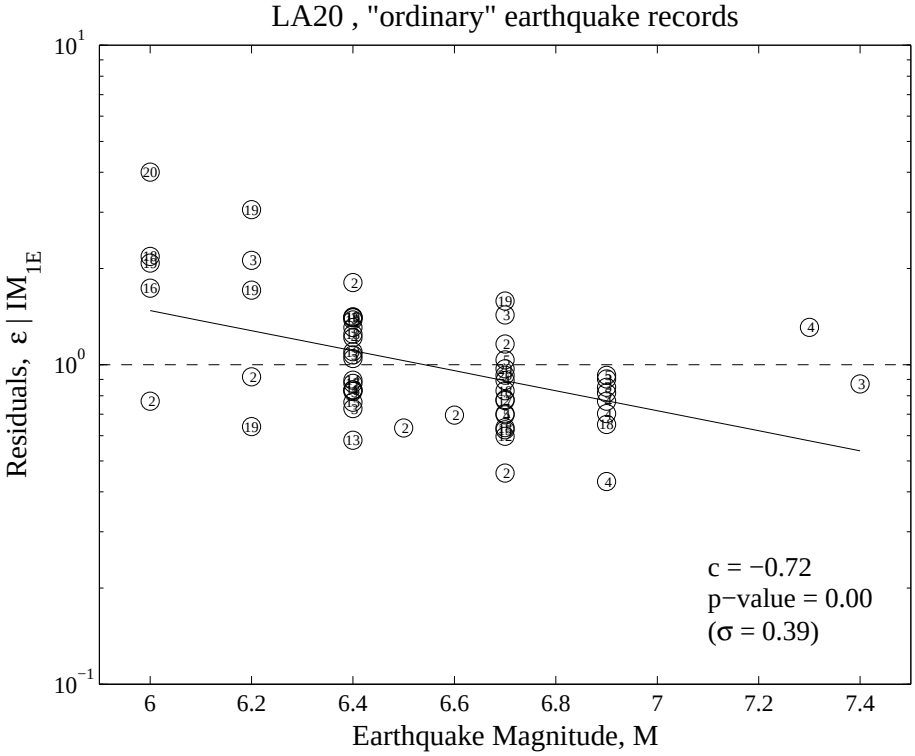

Figure 2. Regression of $\varepsilon|IM_{1E}$ (residuals from Figure 1) on M, in order to quantify the sufficiency of IM_{1E} with respect to M (p–value).

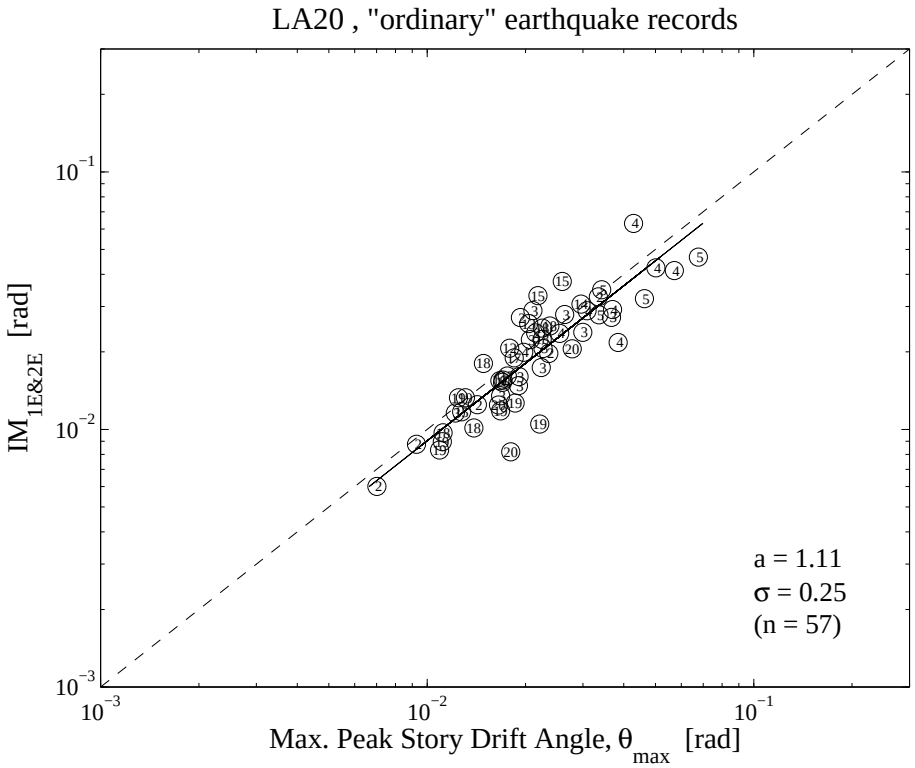

Figure 3. Regression of θ_{max} (from NDA) on ground motion intensity measure $IM_{1E\&2E}$, in order to quantify the bias (a) and efficiency (σ) of $IM_{1E\&2E}$.

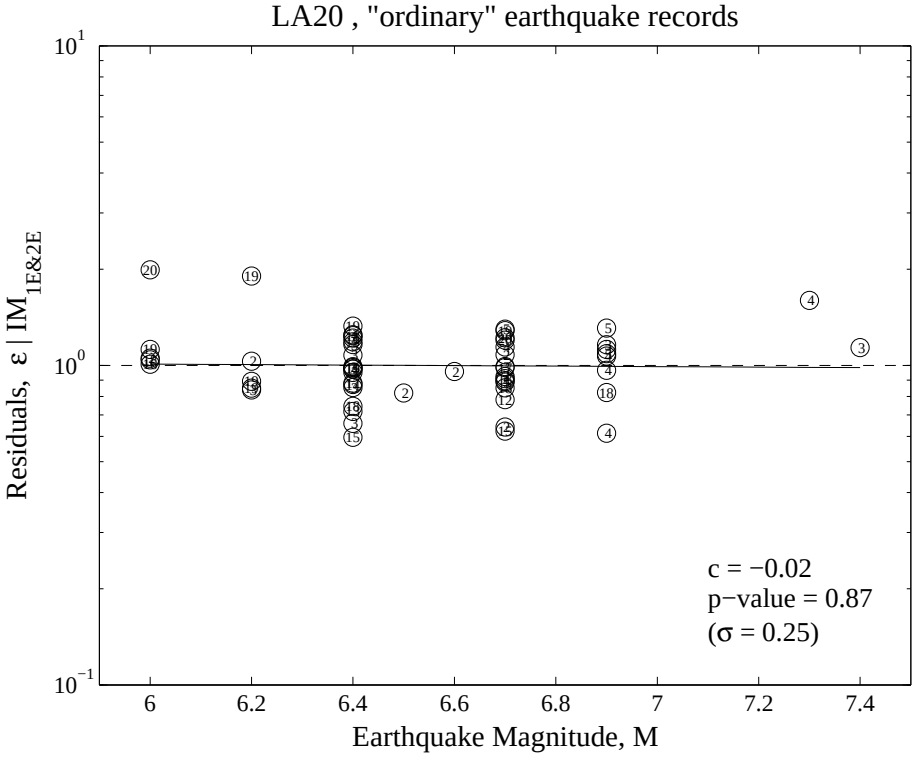

Figure 4. Regression of $\varepsilon|IM_{1E\&2E}$ (residuals from Figure 3) on M, in order to quantify the sufficiency of $IM_{1E\&2E}$ with respect to M (p–value).

considered in order to estimate a with less than 10% variability (i.e., $\sigma_a \leq 0.10$). To the extent that σ reflects the earthquake record-to-record variability of spectral shape (e.g., the $S_d(T_2,\zeta_2)$ to $S_d(T_1,\zeta_1)$ ratio), the inefficiency of IM_{1E} is also (like the bias) due in part to the fact that IM_{1E} does not take into account higher modes.

Notice also from Figure 1 that the residuals about the regression fit (i.e., the observed values of $\varepsilon|IM_{1E}$) appear to be negatively correlated with IM_{1E} (i.e., $\varepsilon|IM_{1E}>1$ for smaller values of IM_{1E}, and vice-versa since by definition the median $\varepsilon|IM_{1E}$ is 1). In turn, IM_{1E} is expected to be positively correlated with M, since the range of R is relatively narrow (i.e., 30 to 46 km). Accordingly, a negative correlation between $\varepsilon|IM_{1E}$ and M is expected, which would imply that IM_{1E} is insufficient; this is confirmed by Figure 2, which shows a significant (p–value $\cong 0$) negative ($c = -0.72$) dependence of $\varepsilon|IM_{1E}$ on M. Although not shown here with a figure, a mild (p–value=0.06) positive ($c = 0.92$) dependence of $\varepsilon|IM_{1E}$ on R is also observed, further suggesting that IM_{1E} is insufficient.

Because the response of the LA20 building model to each of the smaller M earthquake records is roughly elastic, the relatively large values of $\varepsilon|IM_{1E}$ observed in Figure 2 at smaller values of M can be explained by the fact that IM_{1E} does not take into account higher modes. First note that, due to their relatively weak low-frequency content, for smaller M earthquake ground motions the ratio of the spectral displacement at a relatively short period (e.g., corresponding to a higher mode) to that at a longer period (e.g., T_1 for LA20) is on average relatively large (Abrahamson and Silva 1997). Thus, smaller M earthquake records will tend to excite the higher modes relatively more (than larger M earthquake records), resulting in relatively large values of $\varepsilon|IM_{1E}$ because IM_{1E} only considers the first mode. This relatively large contribution of higher modes for smaller M earthquake ground motions is consistent with (or perhaps compounded by) the observation for such earthquake records that $\theta_{\max}$ tends to occur in the upper stories (as seen in Figure 2), where (for example) the second-mode participation factor is relatively large.

In contrast to IM_{1E}, recall that the intensity measure $IM_{1E\&2E}$ takes into account the contribution to $\theta_{\max}$ from the second mode (in addition to the first mode). As evidenced by Figure 3, $IM_{1E\&2E}$ manages to capture much of the higher-mode contribution that resulted in large $\varepsilon|IM_{1E}$ residuals in (or near) the elastic range in Figure 1. Accordingly, the estimated regression coefficient (a=1.11) indicates that $IM_{1E\&2E}$ is only slightly biased in estimating $\theta_{\max}$, and the relatively small scatter about the regression fit (quantified by $\sigma = 0.25$) indicates that $IM_{1E\&2E}$ is substantially more efficient than IM_{1E}. Furthermore, the $\varepsilon|IM_{1E\&2E}$ residuals about the regression fit are more uniformly distributed over the range of $\theta_{\max}$ than are the $\varepsilon|IM_{1E}$ residuals. In fact, as shown in Figure 4, $\varepsilon|IM_{1E\&2E}$ is not significantly dependent on M (p–value=0.87). Although not shown here with a figure, the residuals are also practically independent of R as well (p–value=0.19), suggesting that $IM_{1E\&2E}$ is practically sufficient.

IM_{1I} VS. IM_{1E} (FOR LA3 UNDER NEAR-SOURCE GROUND MOTIONS)

As explained above, it is suspected that $S_a(T_1)$, or equivalently IM_{1E}, may also be relatively inefficient and insufficient when considering the inelastic response (of moderate-period structures) to near-source ground motions. This shortcoming of IM_{1E}, as well as the relative efficiency and sufficiency of IM_{1I} (which accounts for inelasticity), are demonstrated here with the LA3 building model subjected to the 31 near-source earthquake records.

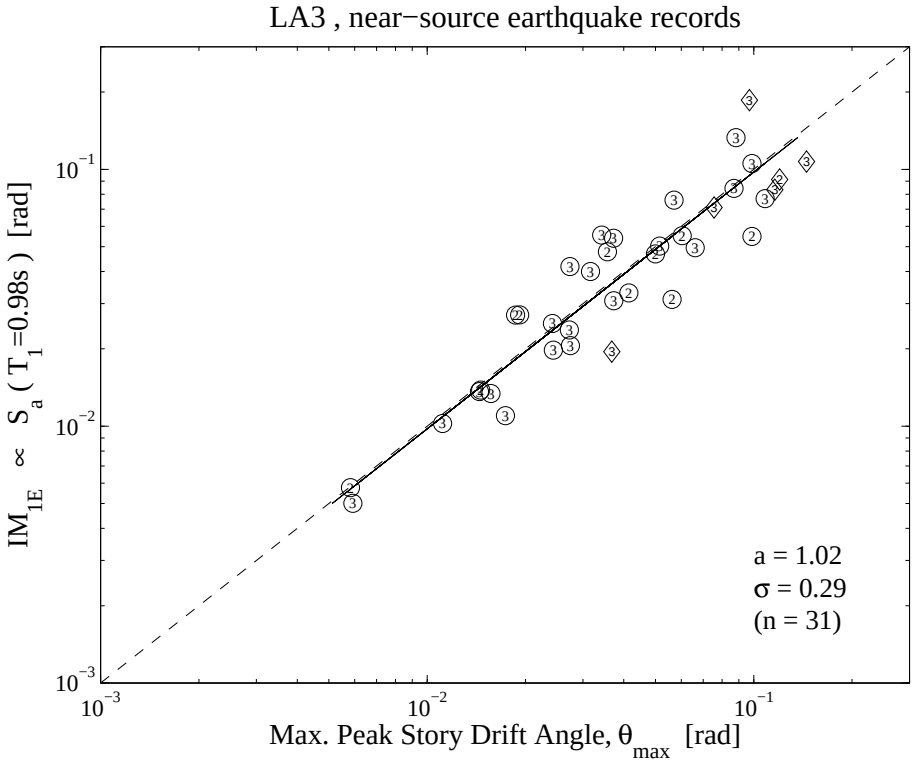

Figure 5. Regression of θ_{max} (from NDA) on ground motion intensity measure IM_{1E}, in order to quantify the bias (a) and efficiency (σ) of IM_{1E}.

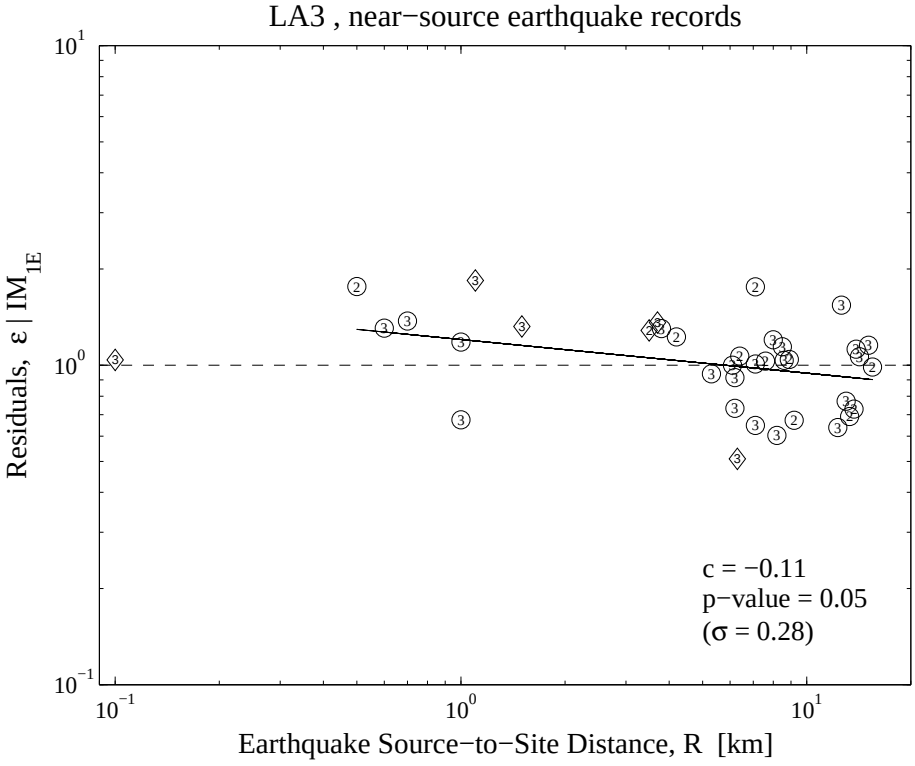

Figure 6. Regression of $\varepsilon|IM_{1E}$ (residuals from Figure 5) on R, in order to quantify the sufficiency of IM_{1E} with respect to R (p–value).

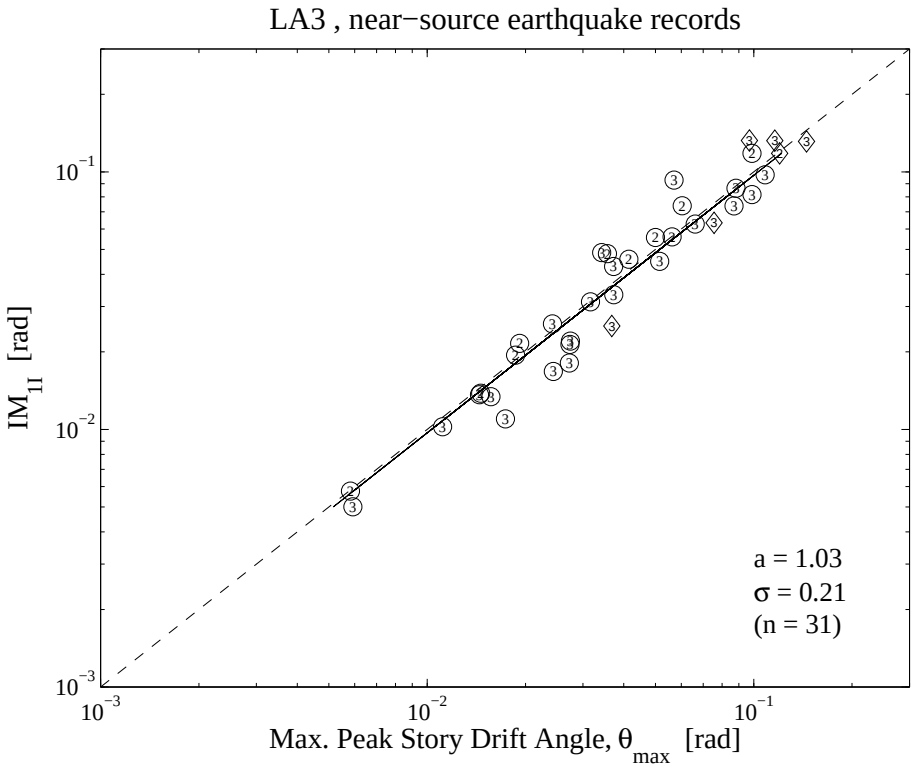

Figure 7. Regression of θ_{max} (from NDA) on ground motion intensity measure IM_{1I}, in order to quantify the bias (a) and efficiency (σ) of IM_{1I}.

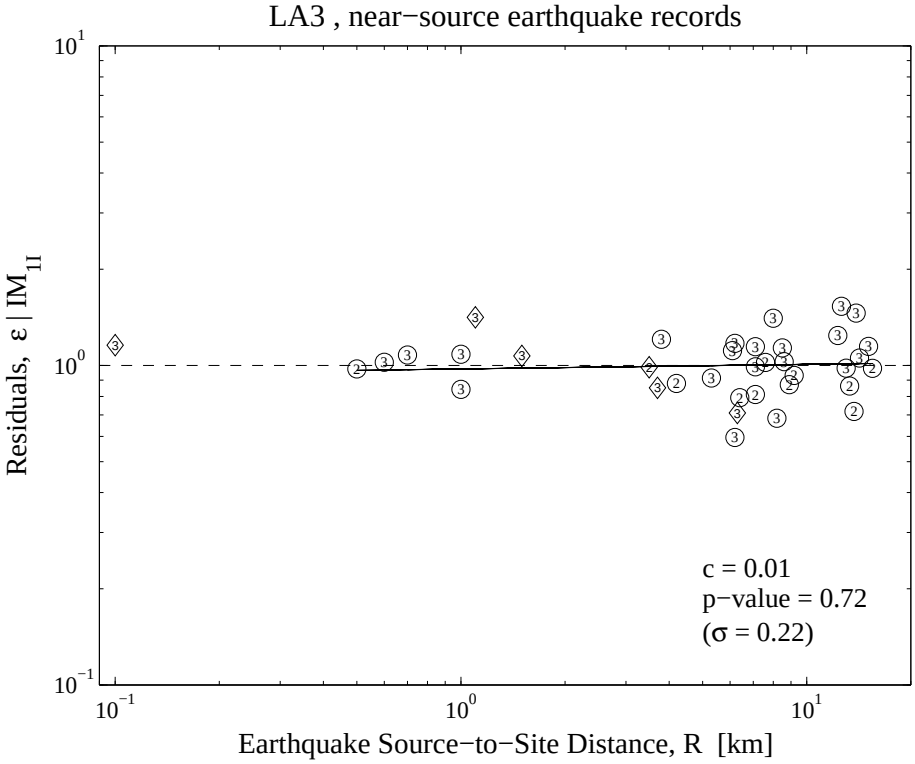

Figure 8. Regression of $\varepsilon|IM_{1I}$ (residuals from Figure 7) on R, in order to quantify the sufficiency of IM_{1I} with respect to R (p–value).

The regression of θ_{max} on IM_{1E} is illustrated in Figure 5. The estimated regression coefficient (a=1.02) indicates that IM_{1E} is essentially unbiased, and the rather small scatter about the regression fit (quantified by σ=0.29) indicates that IM_{1E} is fairly efficient. Note that the data points for the 6 supplemental "pulse-like" earthquake records (symbolized as diamonds), which are not included in the regression analysis, do appear to lie within the scatter of the data for the other 31 near-source earthquake records. The fact that IM_{1E} is essentially unbiased and relatively efficient is not surprising insofar as the response of the LA3 building model is dominated by its first mode (at least in the elastic range). Nevertheless, it does not follow that IM_{1E} is sufficient. As shown in Figure 6, a somewhat mild (p–value=0.05) negative (c= –0.11) dependence of the $\varepsilon|IM_{1E}$ residuals on R is observed. The values of $\varepsilon|IM_{1E}$ for the 6 supplemental pulse-like earthquake records (not included in the regression analysis) appear to support the observed negative dependence. A negative dependence of $\varepsilon|IM_{1E}$ on R is expected to the degree that ground motions at smaller R are more likely to be strongly pulse-like and therefore are more likely to induce large inelastic displacements relative to IM_{1E} (i.e., large values of $\varepsilon|IM_{1E}$). Bear in mind that the dependence on R observed here may be somewhat mild because all of the ground motions considered are near-source (i.e., R<16km).

Although not shown here with a figure, a somewhat significant (p–value=0.02) negative (c= –1.13) dependence of $\varepsilon|IM_{1E}$ on M is also observed. However, recall that of the 31 near-source earthquake records, 14 are from the M=6.5 Imperial Valley earthquake (of 1979), 16 are from the M=6.7 Northridge (1994) and Superstition Hills (1987) earthquakes, and 1 is from the M=6.9 Loma Prieta earthquake (1989). Due to the small number of distinct earthquake events (over a narrow range of M), the results of the regression of $\varepsilon|IM_{1E}$ on M may be suspect. Furthermore, the results for the 6 supplemental pulse-like earthquake records (including 1 from each of the M=6.2 Morgan Hill (1984) and M=7.3 Landers (1992) earthquakes) do not support the observed negative dependence on M. If anything, a positive dependence of $\varepsilon|IM_{1E}$ on M is expected, as explained above in the section on recent studies. Nevertheless, whether due to a dependence on R or M, the regression analysis results suggest that IM_{1E} is relatively insufficient.

Unlike IM_{1E}, recall that the intensity measure IM_{1I} takes into account the effects of inelasticity. The regression of θ_{max} on IM_{1I} is illustrated in Figure 7. As for IM_{1E}, the estimated regression coefficient (a=1.03) indicates that IM_{1I} is essentially unbiased. The small scatter about the regression fit (quantified by σ=0.21) indicates that IM_{1I} is even more efficient than IM_{1E}. Moreover, Figure 8 shows that the $\varepsilon|IM_{1I}$ residuals are not significantly dependent on R (p–value=0.72); although not shown here with a figure, the residuals are also observed to be practically independent of M as well (p–value=0.14), suggesting that IM_{1I} is relatively sufficient. Note that the data for the 6 supplemental pulse-like earthquake records further supports the observations that IM_{1I} is essentially unbiased, more efficient than IM_{1E}, and relatively sufficient.

$IM_{1I\&2E}$ VS. IM_{1E} (FOR LA9 UNDER ORDINARY & NEAR-SOURCE GROUND MOTIONS)

In the previous two subsections, it has been demonstrated that (a) an intensity measure that takes into account higher modes, like $IM_{1E\&2E}$, can be more efficient and sufficient than IM_{1E} if higher modes contribute significantly to the structural response (e.g., LA20), and (b) an intensity measure that takes into account inelasticity, like IM_{1I}, can be more efficient and sufficient than IM_{1E} if inelasticity significantly affects the response, as it does under near-source ground motions for moderate period structures (e.g., LA3). Here the relative

(compared to IM_{1E}) efficiency and sufficiency of $IM_{1I\&2E}$, which takes into account both the second mode and inelasticity, are demonstrated with the LA9 building model subjected both to the ordinary and to the near-source earthquake records. Note that for the first-mode dominated LA3 building model, $IM_{1I\&2E}$ is essentially equivalent to IM_{1I}; for the relatively long period LA20 building model, $IM_{1I\&2E}$ is expected to be (according to the "equal displacements rule") comparable to $IM_{1E\&2E}$ (perhaps even for near-source ground motions). The regression analysis results for the LA3 and LA20 building models, which for the most part confirm these expectations, are summarized in a subsection below (see Table 5).

The LA9 regression analysis results for both IM_{1E} and $IM_{1I\&2E}$ are summarized in Table 2. For both the ordinary and near-source ground motions, the regression estimates of the coefficient a (all approximately 1.2 or larger) indicate that both intensity measures are somewhat biased low in estimating $\theta_{\max}$. Note however, that $IM_{1I\&2E}$ is less biased (i.e., a closer to 1) than IM_{1E}, particularly for the near-source ground motions. Also note that whereas the regression estimates of a are somewhat different for the ordinary versus near-source ground motions when IM_{1E} is employed (i.e., a=1.22 vs. 1.38), they are more similar for $IM_{1I\&2E}$ (i.e., a=1.17 vs. 1.23). As discussed further in Appendix I, this bias similarity is related to the sufficiency of $IM_{1I\&2E}$ relative to IM_{1E}. Moreover, the regression estimates of σ reveal that $IM_{1I\&2E}$ is significantly more efficient than IM_{1E} for both the ordinary (σ=0.27 vs. 0.46) and near-source (σ=0.20 vs. 0.35) earthquake records. Based on the regression estimates of σ and Equation 9, only about 1/3 the number of (ordinary or near-source) earthquake records are needed to estimate the regression coefficient a with $\sigma_a \leq 0.10$ when $IM_{1I\&2E}$ is employed in lieu of IM_{1E}.

Table 2. Regression analysis results for LA9 comparing the bias, efficiency, and sufficiency of the ground motion intensity measures $IM_{1I\&2E}$ and IM_{1E}.

IM	$\theta_{\max}$ on IM		$\varepsilon\|IM$ on M			$\varepsilon\|IM$ on R		
	a	σ	c	p-value	σ	c	p-value	σ
(a) 59 "ordinary" earthquake records								
IM_{1E}	1.22	0.46	-0.46	0.02	0.44	0.53	0.29	0.46
$IM_{1I\&2E}$	1.17	0.27	-0.08	0.51	0.27	0.36	0.22	0.27
(b) 31 near-source earthquake records								
IM_{1E}	1.38	0.35	-0.58	0.31	0.35	-0.03	0.61	0.35
$IM_{1I\&2E}$	1.23	0.20	-0.36	0.26	0.19	-0.02	0.68	0.20

Also listed in Table 2, the p–values suggest that whereas IM_{1E} is rather insufficient for the ordinary earthquake records, $IM_{1I\&2E}$ is relatively sufficient. For the near-source earthquake records, both IM_{1E} and $IM_{1I\&2E}$ are found to be acceptably sufficient. Note that the insufficiency of IM_{1E} for the ordinary earthquake records is due to a somewhat significant (p–value=0.02) negative (c= –0.46) dependence of $\varepsilon|IM_{1E}$ on M, as was observed (above) for the LA20 building model. However, in this case, merely taking into account the elastic contributions to $\theta_{\max}$ of first two modes (i.e., $IM_{1E\&2E}$) does not achieve a sufficient intensity measure for the LA9 building model as it did for the LA20 building model (refer to Table 5 below). Evidently, the effects of inelasticity, in addition to the second mode, must be taken into account in order to achieve a sufficient intensity measure (i.e., $IM_{1I\&2E}$) for the moderate height LA9 building model.

IM_{1eq} VS. IM_{1I} (FOR LA3 UNDER ORDINARY & NEAR-SOURCE GROUND MOTIONS)

As detailed above (i.e., Equation 6), IM_{1eq} is an "equivalent" elastic approximation of IM_{1I} (i.e., one that avoids nonlinear SDOF time-history analysis). Here, the efficiency and sufficiency (as well as the bias) of IM_{1eq} relative to IM_{1I} are demonstrated for the LA3 building model. Whereas above IM_{1I} was compared with IM_{1E} for the LA3 building model subjected to only the near-source earthquake records, here both the ordinary and near-source earthquake records are considered.

The regression analysis results for both IM_{1eq} and IM_{1I} are summarized in Table 3. For both the ordinary and near-source ground motions, the regression estimates of the coefficient a indicate that, whereas IM_{1I} is essentially unbiased in estimating $\theta_{\max}$ ($a\approx1.0$), IM_{1eq} is slightly biased ($a\approx1.1$). Nevertheless, the regression estimates of σ indicate that IM_{1eq} is nearly as efficient as IM_{1I}, for both the ordinary (σ=0.28 vs. 0.25) and near-source (σ=0.22 vs. 0.21) ground motions. The p–values, however, suggest that whereas IM_{1I} is practically sufficient for the near-source earthquake records (as discussed above), IM_{1eq} is somewhat insufficient; for the ordinary earthquake records, both IM_{1eq} and IM_{1I} are evidently sufficient.

Table 3. Regression analysis results for LA3 comparing the bias, efficiency, and sufficiency of of the ground motion intensity measures IM_{1eq} and IM_{1I}.

IM	$\theta_{\max}$ on IM		$\varepsilon\|IM$ on M			$\varepsilon\|IM$ on R		
	a	σ	c	p-value	σ	c	p-value	σ
(a) 59 "ordinary" earthquake records								
IM_{1I}	1.01	0.25	-0.05	0.63	0.25	-0.11	0.70	0.25
IM_{1eq}	1.13	0.28	0.01	0.95	0.28	0.23	0.45	0.28
(b) 31 near-source earthquake records								
IM_{1I}	1.03	0.21	-0.51	0.14	0.21	0.01	0.72	0.22
IM_{1eq}	1.13	0.22	-0.71	0.04	0.21	-0.07	0.09	0.21

The reason why IM_{1eq} is insufficient for the near-source but not the ordinary ground motions probably lies in the details of how the equivalent period and damping ratio for $S_d^{eq}(T_1,\zeta_1,d_y)$ (in Equation 8 for IM_{1eq}) are established. Recall that in determining the equivalent period and damping ratio, $\mu=S_d^I(T_1,\zeta_1,d_y)/d_y$ is approximated with $S_d(T_1,\zeta_1)/d_y$. However, as demonstrated above and in recent studies, $S_d^I(T_1,\zeta_1,d_y)$ can be considerably larger than $S_d(T_1,\zeta_1)$ under near-source ground motions for moderate values of T_1 (e.g., T_1=0.98sec for LA3), and the difference between $S_d^I(T_1,\zeta_1,d_y)$ and $S_d(T_1,\zeta_1)$ may depend on M and/or R. For the LA3 building model, this implies that IM_{1eq} may be insufficient for near-source ground motions; for ordinary ground motions, in contrast, IM_{1eq} may be sufficient because the "equal displacements rule" is more applicable. Particularly for near-source ground motions, μ can be estimated more accurately by updating it with each new calculation of $S_d^{eq}(T_1,\zeta_1,d_y)$ (i.e., computing IM_{1eq} iteratively), but this would make it considerably more difficult to compute $\lambda[IM_{1eq}]$, as discussed briefly below. Moreover, note that the empirical equations used to determine the equivalent period and damping ratio (as a function of μ) were based predominantly on ordinary earthquake records (Iwan 1980); as a result, the effects of inelasticity under near-source ground motions may not be captured properly by $S_d^{eq}(T_1,\zeta_1,d_y)$.

IM_{1eff} VS. IM_{1I} (FOR LA3 UNDER ORDINARY & NEAR-SOURCE GROUND MOTIONS)

Like IM_{1eq}, IM_{1eff} can be considered an approximation of IM_{1I}. However, IM_{1eff} involves only the elastic spectral displacements at T_1 and at a single period longer than T_1 (meant to reflect a reduction in stiffness due to inelasticity). As for IM_{1eq} in the previous subsection, here the efficiency and sufficiency (as well as the bias) of IM_{1eff} relative to IM_{1I} are demonstrated for the LA3 building model subjected to the ordinary and near-source earthquake records.

The regression analysis results for both IM_{1eff} and IM_{1I} are summarized in Table 4. For both the ordinary and near-source ground motions, the regression estimates of the coefficient a indicate that, like IM_{1I}, IM_{1eff} is essentially unbiased in estimating $\theta_{\max}$ (i.e., $a \approx 1.0$). The regression estimates of σ indicate that IM_{1eff} is also nearly as efficient as IM_{1I}, although more-so for the near-source than the ordinary ground motions. Again like IM_{1I}, the p–values suggest that IM_{1eff} is practically sufficient for the near-source ground motions. However, whereas IM_{1I} is also sufficient for the ordinary ground motions, IM_{1eff} is evidently somewhat insufficient due to a mild (p–value=0.05) negative (c=–0.25) dependence of $\varepsilon|IM_{1eff}$ on M.

Table 4. Regression analysis results for LA3 comparing the bias, efficiency, and sufficiency of the ground motion intensity measures IM_{1eff} and IM_{1I}.

IM	$\theta_{\max}$ on IM		$\varepsilon\|IM$ on M			$\varepsilon\|IM$ on R		
	a	σ	c	p-value	σ	c	p-value	σ
(a) 59 "ordinary" earthquake records								
IM_{1I}	1.01	0.25	-0.05	0.63	0.25	-0.11	0.70	0.25
IM_{1eff}	0.98	0.30	-0.25	0.05	0.29	-0.04	0.90	0.30
(b) 31 near-source earthquake records								
IM_{1I}	1.03	0.21	-0.51	0.14	0.21	0.01	0.72	0.22
IM_{1eff}	0.97	0.23	-0.05	0.89	0.23	-0.06	0.15	0.22

The relatively large values of $\varepsilon|IM_{1eff}$ for smaller values of M that are implied by the negative dependence observed for the ordinary earthquake records may be explained by a known deficiency of IM_{1eff} in the realm of elastic response. Recall from Equation 7 that IM_{1eff} is the product of IM_{1E} and a modification factor that reflects the ratio of the spectral displacement at $2T_1$ to that at T_1. In the event of elastic response, IM_{1E} alone is nearly unbiased in estimating $\theta_{\max}$ for a first-mode dominated building model like LA3. However, for the smaller M earthquake records that most often result in elastic response, IM_{1eff} on average under-estimates $\theta_{\max}$ because the ratio of $S_d(2T_1,\zeta_1)$ to $S_d(T_1,\zeta_1)$ is typically relatively small for such ground motions (Abrahamson and Silva 1997). In other words, relatively large values of $\varepsilon|IM_{1eff}$ are expected for smaller values of M. For the near-source earthquake records, recall that a dependence on M is difficult to observe due to the narrow range of M (i.e., 6.5 to 6.9).

SUMMARY OF RESULTS

The regression analysis results for the four primary intensity measures IM_{1E}, $IM_{1E\&2E}$, IM_{1I}, and $IM_{1I\&2E}$ are summarized in Table 5 for every combination of the three building models (LA3, LA9, and LA20) and two suites of earthquake records (ordinary and near-

source). Note that only some of the results listed in the table are described in detail in the subsections above; a complete description is left to (Luco 2001). Nevertheless, many of the results listed in Table 5 are referred to in the following sections.

Table 5. Summary of regression analysis results comparing the bias, efficiency, and sufficiency of the four "primary" ground motion intensity measures.

IM	$\theta_{\max}$ on *IM*		$\varepsilon\|IM$ on *M*			$\varepsilon\|IM$ on *R*		
	a	σ	*c*	*p*-value	σ	*c*	*p*-value	σ
(a) LA3 subjected to 59 "ordinary" earthquake records								
IM_{1E}	0.84	0.28	-0.28	0.02	0.27	-0.03	0.92	0.28
$IM_{1E\,\&\,2E}$	0.83	0.27	-0.26	0.03	0.26	-0.06	0.85	0.27
IM_{1I}	1.01	0.25	-0.05	0.63	0.25	-0.11	0.70	0.25
$IM_{1I\,\&\,2E}$	0.99	0.24	-0.03	0.78	0.24	-0.13	0.62	0.24
(b) LA3 subjected to 31 near-source earthquake records								
IM_{1E}	1.02	0.29	-1.13	0.02	0.27	-0.11	0.05	0.28
$IM_{1E\,\&\,2E}$	1.01	0.28	-1.01	0.02	0.26	-0.12	0.02	0.26
IM_{1I}	1.03	0.21	-0.51	0.14	0.21	0.01	0.72	0.22
$IM_{1I\,\&\,2E}$	1.01	0.19	-0.40	0.21	0.19	0.00	0.95	0.20
(c) LA9 subjected to 59 "ordinary" earthquake records								
IM_{1E}	1.22	0.46	-0.46	0.02	0.44	0.53	0.29	0.46
$IM_{1E\,\&\,2E}$	0.99	0.32	-0.37	0.01	0.31	0.82	0.02	0.31
IM_{1I}	1.44	0.37	-0.17	0.29	0.37	0.07	0.85	0.37
$IM_{1I\,\&\,2E}$	1.17	0.27	-0.08	0.51	0.27	0.36	0.22	0.27
(d) LA9 subjected to 31 near-source earthquake records								
IM_{1E}	1.38	0.35	-0.58	0.31	0.35	-0.03	0.61	0.35
$IM_{1E\,\&\,2E}$	1.19	0.31	-1.51	0.00	0.27	-0.09	0.13	0.31
IM_{1I}	1.43	0.25	0.57	0.16	0.24	0.04	0.41	0.25
$IM_{1I\,\&\,2E}$	1.23	0.20	-0.36	0.26	0.19	-0.02	0.68	0.20
(e) LA20 subjected to 57 "ordinary" earthquake records								
IM_{1E}	1.59	0.44	-0.72	0.00	0.39	0.92	0.06	0.43
$IM_{1E\,\&\,2E}$	1.11	0.25	-0.02	0.87	0.25	0.36	0.19	0.24
IM_{1I}	1.81	0.41	-0.64	0.00	0.36	0.87	0.05	0.40
$IM_{1I\,\&\,2E}$	1.26	0.29	0.07	0.60	0.29	0.31	0.33	0.29
(f) LA20 subjected to 30 near-source earthquake records								
IM_{1E}	1.70	0.37	0.69	0.26	0.36	-0.05	0.48	0.37
$IM_{1E\,\&\,2E}$	1.50	0.32	-0.14	0.79	0.33	-0.08	0.18	0.31
IM_{1I}	1.92	0.31	0.78	0.12	0.30	-0.10	0.07	0.29
$IM_{1I\,\&\,2E}$	1.69	0.28	-0.05	0.92	0.29	-0.13	0.01	0.25

DISCUSSION

As mentioned in the introduction, the only perfectly efficient and sufficient (not to mention unbiased) ground motion intensity measure is *DM* itself. Defining *IM* equal to *DM* would entirely eliminate the need to estimate $G[DM|IM]$ and to integrate over *IM* in Equation 1 for $\lambda[LS]$. However, directly computing the *DM* hazard $\lambda[DM]$ via PSHA would require a structure-specific attenuation relation for *DM*, which in turn would require hundreds of

relatively time-consuming NDA's of the model structure under ground motions from an array of M's and R's. Because the alternative IM's considered in this paper can each be computed with at most a few relatively expeditious SDOF earthquake time-history analyses (once given the modal vibration properties and a NSP curve for the structure), it is more practical to compute $\lambda[IM]$ than $\lambda[DM]$. Obviously, though, none of the alternative IM's are as efficient and sufficient as DM. As discussed here, an analogous trade-off between the efficiency and sufficiency of IM and the computability of $\lambda[IM]$ is also apparent amongst the alternative IM's.

For the most part (as summarized in Table 5), IM_{1E} is relatively inefficient and insufficient in comparison to the other alternative ground motion intensity measures. As a result, a relatively large number of NDA's and site-specific seismicity information (i.e., $dG[M,R|IM_{1E}]$, as explained in Appendix I) are in general necessary to estimate $G[DM|IM_{1E}]$ accurately. In favor of IM_{1E}, however, the ground motion hazard $\lambda[IM_{1E}]$ can be computed via a common PSHA that makes use of an existing attenuation relation for spectral acceleration (since $S_a(T_1)$ is effectively proportional to IM_{1E}). In a sense, the computation of $\lambda[IM_{1E}]$ can take advantage of the hundreds of SDOF earthquake time-history analyses that were carried out in developing the attenuation relation. Note also that $\lambda[S_a(T_1)]$ and thereby $\lambda[IM_{1E}]$ may already be available for the designated site (e.g., from the U.S. Geological Survey at http://geohazard.cr.usgs.gov/eq/).

In contrast to IM_{1E}, for the most part $IM_{1I\&2E}$ is found to be relatively efficient and sufficient (again, as summarized in Table 5). Thus, $G[DM|IM_{1I\&2E}]$ can be estimated with relatively few NDA's and without site-specific seismicity information. However, as attenuation relations for inelastic spectral displacement are not yet available, computing the ground motion hazard $\lambda[IM_{1I\&2E}]$ (or $\lambda[IM_{1I}]$ for that matter) via PSHA currently requires hundreds of inelastic SDOF time-history analyses. Otherwise, conceptually there is little difference between computing $\lambda[IM_{1I\&2E}]$ (or $\lambda[IM_{1I}]$) and $\lambda[IM_{1E}]$, and neither involves the hundreds of NDA's of the given MDOF structure that would be necessary to directly compute $\lambda[DM]$ via PSHA. Perhaps in the near future, attenuation relations for inelastic spectral displacement will be developed, facilitating a PSHA for $IM_{1I\&2E}$ (or IM_{1I}). Note, incidentally, that in addition to being relatively efficient and sufficient, $IM_{1I\&2E}$ (or IM_{1I}) is unbiased for the LA3 building model. In general, such an unbiased and efficient intensity measure might be treated as an approximate DM, an option pursued further in (Luco 2001).

Although (even in comparison to $IM_{1I\&2E}$) the intensity measure $IM_{1E\&2E}$ is found to be relatively efficient and sufficient for the LA20 building model, it is relatively inefficient and insufficient for the LA3 and LA9 building models (as evidenced by Table 5). In computing the ground motion hazard via PSHA, though, the advantage of $IM_{1E\&2E}$ is that existing attenuation relations for $S_a(T_1)$ and $S_a(T_2)$ can be combined in order to approximate an attenuation relation for $IM_{1E\&2E}$. With an attenuation relation for $IM_{1E\&2E}$, the ground motion hazard $\lambda[IM_{1E\&2E}]$ can be computed in the same manner as $\lambda[IM_{1E}]$ (i.e., without hundreds of SDOF earthquake time-history analyses). Because of the many possible pairs of modal periods and participation factors, the PSHA carried out to compute $\lambda[IM_{1E\&2E}]$ must, of course, be structure specific. Nonetheless, one can envision a software package or even a U.S. Geological Survey web-site capable of addressing this problem easily.

Analogous to $IM_{1E\&2E}$, the intensity measure IM_{1eq} is merely a (complicated) function of elastic spectral displacements. In fact, IM_{1eq} was introduced as a surrogate for IM_{1I} that could conceivably take advantage of existing attenuation relations for elastic spectral accelerations in computing, in an approximate manner, the ground motion hazard $\lambda[IM_{1eq}]$ via PSHA.

Alternatively, the same elastic response spectra data that is used in developing existing attenuation relations can be used to form an attenuation relation for IM_{1eq}, without re-running hundreds of SDOF time-history analyses; this is true even if IM_{1eq} is computed iteratively (an option mentioned above with the results for IM_{1eq}). In turn, such an attenuation relation for IM_{1eq} can be used to compute $\lambda[IM_{1eq}]$ more accurately. (Note that the same can be done for $IM_{1E\&2E}$, since it too involves only elastic spectral displacements.) Although IM_{1eq} is found (above) to be about as efficient as IM_{1I} for the first-mode dominated LA3 building model, a disadvantage of IM_{1eq} is its relatively insufficient for the near-source earthquake records.

Also somewhat similar to $IM_{1E\&2E}$, the intensity measure IM_{1eff} is (approximately proportional to) a function of $S_a(T_1)$ and $S_a(2T_1)$. Like IM_{1eq}, IM_{1eff} was in fact introduced as a surrogate to IM_{1I} that can take advantage of existing attenuation relations for elastic spectral accelerations in computing the ground motion hazard $\lambda[IM_{1eff}]$ via PSHA. As IM_{1eff} is a log-log linear combination of $S_a(T_1)$ and $S_a(2T_1)$, given an estimate of the correlation between $S_a(T_1)$ and $S_a(2T_1)$ (Sewell 1989) an attenuation relation (median and dispersion) for IM_{1eff} can be easily derived from those for spectral acceleration (Cordova et al 2001). Thus, $\lambda[IM_{1eff}]$ can be estimated nearly as readily as $\lambda[IM_{1E}]$. However, IM_{1eff} is found (above) to be relatively insufficient for the LA3 building model subjected to the ordinary earthquake records. As for IM_{1eq}, apparently the advantage of IM_{1eff} in terms of the computability of its hazard is tempered by its inefficiency and/or insufficiency.

CONCLUSIONS

The investigation of alternative *IM*'s (i.e., ground motion intensity measures) is facilitated by defining the "efficiency" and "sufficiency" of an *IM* that is to be employed in the structural performance assessment scheme summarized in the introduction. As detailed in the approach section, the efficiency and sufficiency of an *IM* are both criteria that can be quantified via regression analysis with *DM* (e.g., drift response) results from nonlinear dynamic analysis (NDA) of a structure. For three different SMRF buildings of moderate-to-long period subjected both to ordinary and to near-source ground motions, the efficiency and sufficiency of six new alternative *IM*'s are compared in this paper.

Especially in comparison to the conventional intensity measure $S_a(T_1)$ (or equivalently IM_{1E}), the ground motion intensity measure denoted $IM_{1I\&2E}$ (which takes into account second-mode frequency content and inelasticity) is demonstrated to be relatively efficient and sufficient in estimating the structural drift response measure $\theta_{\max}$, as summarized in Table 5. This holds true under both the near-source and the ordinary suites of earthquake records for two of the three building models. The lone exception is the tall, long period (T_1=3.96sec) LA20 building model subjected to the near-source earthquake records. In this case, although $IM_{1I\&2E}$ is the most efficient of the four primary intensity measures (listed in Table 5), it is not sufficient due to a significant conditional (given $IM_{1I\&2E}$) dependence of $\theta_{\max}$ on R (i.e., earthquake source-to-site distance). Note that this conditional dependence on R is also apparent from the significant difference in the bias's of $IM_{1I\&2E}$ in estimating $\theta_{\max}$ for the near-source versus the ordinary (or far-field) earthquake records (i.e., a=1.69 vs. 1.26). For the LA3 and LA9 building models, in contrast, the strong similarity of the bias (and the efficiency) of $IM_{1I\&2E}$ for the near-source versus ordinary earthquake records suggests that the relationship between $IM_{1I\&2E}$ and $\theta_{\max}$ is independent of the type of ground motion. In turn, this independence implies that near-source ground motions need not be treated as special cases if the intensity measure $IM_{1I\&2E}$ is employed (for the LA3 and LA9 building models).

Evidently, even $IM_{1I\&2E}$ is not necessarily an efficient and sufficient intensity measure of both near-source and ordinary ground motions for all types of buildings. Of course, there are several options for potentially improving the efficiency and sufficiency of $IM_{1I\&2E}$. For the LA20 building model, for example, the third mode of (elastic) response can be taken into account in addition to the first and second modes. Moreover, the inelastic spectral displacement considered for the first-mode can be computed for a trilinear oscillator (i.e., EPP followed by a negative stiffness) or even a bilinear oscillator with negative post-yield stiffness. The backbone curve of either of these two oscillators is more compatible with the nonlinear static pushover curve for the LA20 building model (Luco 2001) than is that of the EPP oscillator utilized for $IM_{1I\&2E}$ in this paper. Yet another possibility is to adjust the (elastic) modal participation factors that are used so as to reflect the effects of P-Δ or a soft story.

Although the options listed above for improving the efficiency and sufficiency of $IM_{1I\&2E}$ have been explored by the authors (Luco 2001), the resulting *IM*'s are not included among those investigated in this paper. Nevertheless, the same approach that is detailed in this paper for quantifying the efficiency and sufficiency (as well as the bias) of an *IM* can be used to appraise any such *IM*'s. Recall (from the discussion section) that, besides the efficiency and sufficiency of an *IM*, it is also important to consider the computability of the ground motion hazard in terms of *IM* (which is put to use in the structural performance assessment scheme). Altogether, a basis for comparing and selecting appropriate ground motion intensity measures for a given structure has been demonstrated.

ACKNOWLEDGEMENTS

The authors gratefully acknowledge the financial support of the U.S.-Japan Cooperative Research in Urban Earthquake Disaster Mitigation Project (NSF 98-36) under grant number CMS-9821096, and the PEER Center (also sponsored by NSF) under project number 3051999.

APPENDIX I: SUFFICIENCY

As stated in the introduction, a "sufficient" *IM* is desirable because it ensures that the scheme expressed by Equation 1 will result in an "accurate" estimate of $\lambda[LS]$ for a given structure at a designated site. Equation 1 for $\lambda[LS]$ is merely an application of the "total probability theorem," so theoretically the result should be the same regardless of the choice of *IM* (or *DM*). However, (as mentioned above) $G[DM|IM]$ in Equation 1 is normally estimated using NDA results for a limited number of earthquake ground motion records. If *IM* is not sufficient (i.e., if *DM* is not conditionally independent, given *IM*, of *M* and *R*), then the estimate of $G[DM|IM]$ must be expected to depend to some degree on the *M*'s and *R*'s of the earthquake records selected. In this (insufficient *IM*) case, unless the distribution of the *M*'s and *R*'s (conditioned on *IM*) of the selected ground motions matches the distribution that appears naturally at the site (as discussed in more detail below), the estimate of $G[DM|IM]$ and thereby of $\lambda[LS]$ (by Equation 1) will be somewhat inaccurate. In contrast, if *IM* is sufficient, by definition the $G[DM|IM]$ estimate will be independent of the *M*'s and *R*'s of the selected ground motions, and therefore $\lambda[LS]$ estimated with Equation 1 should be accurate, in principle, *regardless* of which earthquake records are used to estimate $G[DM|IM]$.

As an example demonstrating that the estimate of $G[DM|IM]$ can depend on the *M*'s of the selected ground motions if *IM* is not sufficient, consider the *DM* (here $\theta_{\max}$) on *IM*

regression results summarized in Table 6 for the LA9 building model subjected to the "ordinary" earthquake records with M<6.5 versus those with M≥6.5. Recall that $G[DM|IM]$ is to be estimated from these regression results (under the assumption that DM is log-normally distributed given IM); thus, different regression results will lead to different estimates of $G[DM|IM]$. From Table 6, notice that for IM_{1E}, which was found (above) to be insufficient for the LA9 building model subjected to the ordinary earthquake records, the regression estimate of the parameter a using the ordinary earthquake records with M<6.5 is different from that using the earthquake records with M≥6.5 (i.e., a=1.33 vs. 1.13). (The two regression estimates of σ for IM_{1E} happen to be approximately equal.) In contrast, for $IM_{1I\&2E}$, which was found to be sufficient (for LA9 subjected to the ordinary earthquake records), the estimates of a and σ are approximately equal for the two subsets of the ordinary earthquake records partitioned by M.

Table 6. $\theta_{\max}$ on IM regression results for LA9 demonstrating a dependence on M for the relatively insufficient IM_{1E} but not for the relatively sufficient $IM_{1I\&2E}$.

IM	a	σ
(a) 29 "ordinary" earthquake records of M < 6.5		
IM_{1E}	1.33	0.45
$IM_{1I\&2E}$	1.18	0.28
(b) 30 "ordinary" earthquake records of M ≥ 6.5		
IM_{1E}	1.13	0.46
$IM_{1I\&2E}$	1.15	0.26

In other words, the $G[DM|IM]$ estimate depends on whether the M<6.5 or the M≥6.5 suite of earthquake records is selected if the insufficient IM_{1E} is employed, but not if the sufficient $IM_{1I\&2E}$ is used. (It follows that different combinations of the earthquake records from the two suites would also lead to different estimates of $G[DM|IM]$ if the insufficient IM_{1E} is employed.) Also for the LA9 building model, recall that a difference in the regression estimates of a for the near-source versus ordinary suites of earthquake records was noted (above) for the insufficient IM_{1E}, but not (to the same extent) for the sufficient $IM_{1I\&2E}$. These regression results (listed in Table 2) demonstrate a dependence of the estimate of $G[DM|IM]$ on, in this case, the R's of the selected ground motions for an insufficient IM.

In order to accurately estimate $\lambda[LS]$ even if IM is insufficient and a limited number of earthquake records are used to estimate $G[DM|IM]$, the dependence on M and R (e.g., as demonstrated above) can be accounted for explicitly. Analogous to Equation 1, $\lambda[LS]$ can be expressed as an application of the total probability theorem that integrates over not only DM and IM, but over M and R as well, as in Equation 12.

$$\lambda[LS] = \iiiint_{DM,\,IM,\,M,\,R} G[LS \mid DM] \,|\, \mathrm{d}G[DM \mid IM, M, R] \,|\, |\, \mathrm{d}G[M, R \mid IM \,|\, |\, \mathrm{d}\lambda[IM]\,|, \quad (12)$$

Note that formally $G[LS|DM]$ in Equation 12 should be $G[LS|DM,IM,M,R]$, but here the latter is presumed to be functionally independent of IM, M, and R because LS is normally defined in terms of DM only; analogously, $G[LS|DM]$ in fact replaces $G[LS|DM,IM]$ in Equation 1. Unlike Equation 1, Equation 12 for $\lambda[LS]$ is expected to be accurate regardless of whether or not IM is sufficient, and regardless of which earthquake records are selected to estimate $G[DM|IM,M,R]$ (Shome and Cornell 1999). Clearly this accuracy comes at the

expense of having to integrate, over M and R, the product of (a) $G[DM|IM,M,R]$, which calls for (in its estimation) a multidimensional regression of DM on IM, M, and R, and (b) $dG[M,R|IM]$, which is the result of a disaggregation of $\lambda[IM]$ for each value of IM (Bazzurro and Cornell 1999). It should be noted that $dG[M,R|IM]$ is a site-dependent distribution; that is, different events (i.e., M's and R's) typically dominate the IM hazard (i.e., $\lambda[IM]$) at different sites. If IM is sufficient, however, by definition $G[DM|IM,M,R]$ is functionally independent of M and R and hence Equation 12 simplifies to Equation 1 while maintaining its accuracy.

Although it has been affirmed that a sufficient IM ensures the accuracy of Equation 1 for $\lambda[LS]$, employing a sufficient IM is not the only way to this accuracy; two other means are discussed briefly here. As mentioned above, the conditional (on IM) distribution of the M's and R's of the earthquake records selected to estimate $G[DM|IM]$ may match (closely enough) the distribution that appears naturally at the site, namely $dG[M,R|IM]$. Using a suite of earthquake records that is consistent with $dG[M,R|IM]$ (to estimate $G[DM|IM]$) has the effect of carrying out the integration over M and R in Equation 12, thereby resulting in an accurate estimate of $\lambda[LS]$ with Equation 1 even if IM is insufficient. In practice, though, it would be very difficult to select a suite of earthquake records that is consistent with $dG[M,R|IM]$ unless the same events dominate the hazard at all IM levels. When the suite of earthquake records used to estimate $G[DM|IM]$ is *not* consistent with $dG[M,R|IM]$, a weighted regression of DM on IM that adjusts (approximately) for this inconsistency can be conducted in order to estimate $G[DM|IM]$. Such a scheme has been applied by Shome and Cornell (1999, page 208) and Bazzurro (1998, page 285) in order to adjust for the conditional distribution of $S_a(T_2)$ given $S_a(T_1)$, and the same approach can be followed for M (or R) given IM. This weighted regression scheme has the effect of carrying out the integration over M and R in Equation 12; thus, it also results in an accurate estimate of $\lambda[LS]$ with Equation 1 even if IM is insufficient. Note that among all of the alternatives discussed for estimating $\lambda[LS]$ with confident accuracy, only the use of a sufficient IM manages to do so without concern about the nature of the site seismicity (i.e., $dG[M,R|IM]$ from disaggregation of $\lambda[IM]$).

Regarding the definition of a sufficient IM, note that it should theoretically include conditional (given IM) independence of DM not just from M and R (as in this paper), but from all influential parameters. For example, if near-source directivity effects are of concern, the definition of a sufficient IM should include conditional independence of DM from (in addition to M and R) the directivity parameter $X\cos\theta$ (or $Y\cos\phi$) introduced by Somerville et al. (1997a). With the building models and ground motions considered in this paper, however, little evidence of a conditional (given any of the alternative IM's) dependence of DM on this directivity parameter has been encountered (Luco 2001). More generally, the definition of sufficiency should include (at least) those parameters that are taken into account by attenuation relations for IM (e.g., faulting style, soil type, etc.). In the case of soil type, in lieu of demonstrating conditional independence of DM from soil type, the ground motions used to estimate $G[DM|IM]$ may be (and have been in this paper) exclusively selected from those recorded on the same soil type as the designated site.

APPENDIX II: PARTICIPATION FACTORS

The participation factors for $\theta_{\max}$ used in calculating the alternative IM's introduced in this paper are defined here. First, let θ_i denote the peak drift angle for the i^{th} story of a building model. The j^{th}–mode participation factor for θ_i is defined here as

$$PF_j(\theta_i) = \Gamma_j \frac{\phi_{j,i} - \phi_{j,i-1}}{h_i}, \tag{13}$$

where $\phi_{j,i}$ is the element of the j^{th} modal vector that corresponds to the upper floor of the i^{th} story (i.e., the i^{th} floor), and h_i is the height of the i^{th} story (in the same units used for spectral displacement). Γ_j, which is also commonly referred to as a participation factor, is given (Chopra 1995) by

$$\Gamma_j = \sum_{i=1:n} \phi_{j,i} m_i \Big/ \sum_{i=1:n} \phi_{j,i}^2 m_i \ , \tag{14}$$

where n is the total number of stories (or floors) in the building model and m_i is the mass of the i^{th} floor.

With $PF_j(\theta_i)$ defined according to Equation 13, the (elastic) SRSS estimate of θ_i using the first k modes is expressed as

$$\theta_i^{[k]} = \sqrt{\sum_{j=1:k} [PF_j(\theta_i) \cdot S_d(T_j, \zeta_j)]^2} \ , \tag{15}$$

where $S_d(T_j,\zeta_j)$ is the spectral displacement of the SDOF oscillator representing the j^{th} mode. For a specified k, the largest $\theta_i^{[k]}$ (among all the stories, i=1:n) is adopted here as the SRSS estimate of θ_{max}, denoted $\theta_{max}^{[k]}$. Clearly, $\theta_{max}^{[k]}$ corresponds to a particular story, denoted $i^{[k]}$ (which, incidentally, does not necessarily match the story corresponding to the observed θ_{max}). Associated with story $i^{[k]}$ are the participation factors $PF_j(\theta_{max}^{[k]})$, which are formally defined in Equation 16.

$$PF_j(\theta_{max}^{[k]}) = PF_j(\theta_{i^{[k]}}) \qquad \text{where} \qquad i^{[k]} = \arg\max_{i=1:n} \theta_i^{[k]}, \tag{16}$$

Note that with k>1, $PF_j(\theta_{max}^{[k]})$ is different for different earthquake records, as it depends on the values of $S_d(T_j,\zeta_j)$ for each of the k modes (or in other words, the spectral shape). With k=1, on the other hand, Equation 16 simplifies to

$$PF_j(\theta_{max}^{[1]}) = \Gamma_j \max_{i=1:n} \left[\frac{\phi_{j,i} - \phi_{j,i-1}}{h_i} \right], \tag{17}$$

which is independent of the earthquake record. Finally, note that $PF_j(\theta_{max}^{[k]})$ is abbreviated as $PF_j^{[k]}$ in Equations 2-6 for alternative *IM*'s.

APPENDIX III: YIELD DISPLACEMENT

As mentioned above, the yield displacement d_y in $S_d^I(T_1,\zeta_1,d_y)$ or $S_d^{eq}(T_1,\zeta_1,d_y)$, which are used in calculating IM_{1I} and $IM_{1I\&2E}$ or IM_{1eq} (respectively), can be determined via a NSP (nonlinear static-pushover) of the model structure under consideration. The approach is described here generally, and is illustrated in Figure 9 for the LA9 building model. A comparison with other methods of estimating d_y is left to (Luco 2001).

Since d_y is the yield displacement of an SDOF oscillator that represents the first mode of the model structure (i.e., T_1 and ζ_1), a "first-mode lateral load pattern" is applied during the NSP conducted to estimate d_y. A first-mode load pattern is that which, in the elastic range,

results in the first-mode deflected shape of the model structure. Derived from (elastic) modal analysis, the first-mode lateral load applied at the i^{th} floor of a building model, denoted F_i, is given by

$$F_i = \frac{m_i \phi_{1,i}}{V_b \sum_{i=1:n} m_i \phi_{1,i}}, \tag{18}$$

where m_i, $\phi_{1,i}$, and n are defined in Appendix II for Equations 13 and 14, and V_b is the base shear (i.e., sum of F_i for i=1:n).

For this paper, an EPP idealization of the V_b versus θ_{roof} (i.e, roof drift angle) curve resulting from the NSP of the building model (applying the first-mode lateral load pattern defined by F_i) is used to estimate d_y. The elastic slope of the bilinear depiction follows the elastic points of the NSP curve (which, by the way, can be used to establish T_1 because a first-mode load pattern is applied). The perfectly-plastic slope passes through the peak V_b on the NSP curve (e.g., for θ_{roof} between 0 and 0.10). The intersection of the two lines provides an estimate of $(\theta_{roof})_y$, the yield displacement in θ_{roof} terms, which is translated to d_y according to elastic modal analysis by

$$d_y = (\theta_{roof})_y \Big/ \Gamma_1 \frac{\phi_{1,n}}{\sum_{i=1:n} h_i}, \tag{19}$$

where Γ_1, $\phi_{1,n}$, and h_i are defined in Appendix II for Equation 13. The values of d_y estimated by the above approach for the LA3, LA9, and LA20 building models are listed in Table 1.

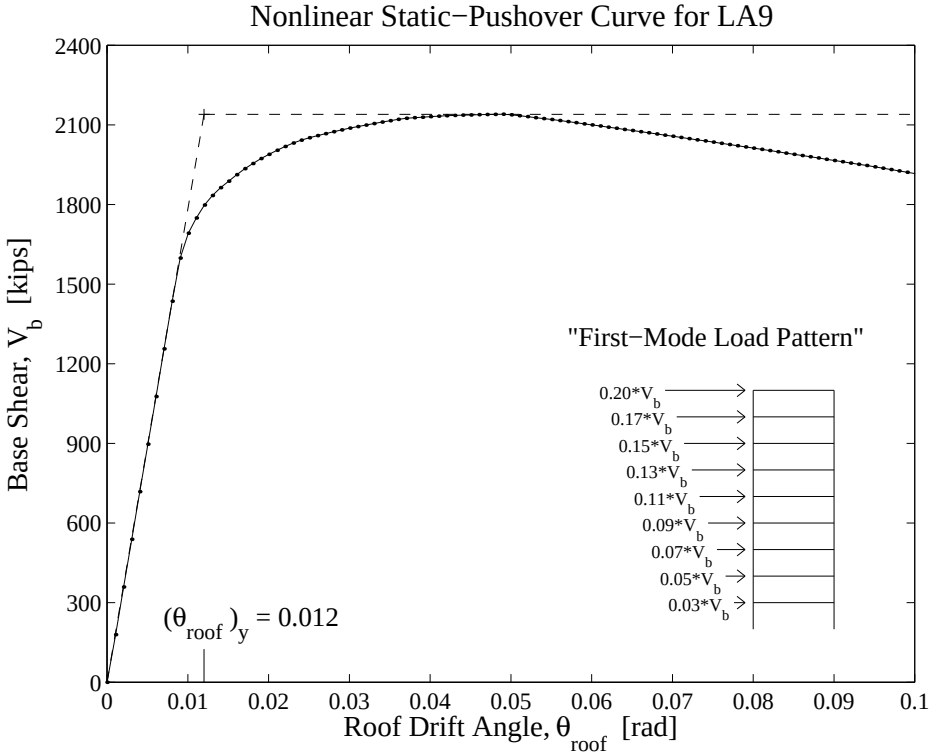

Figure 9. Illustration of procedure for estimating d_y via NSP.

REFERENCES CITED

Abrahamson N.A., Silva W.J., 1997, Empirical response spectral attenuation relations for shallow crustal earthquakes, *Seismological Research Letters*, **68(1)**, 94-127.

Alavi B., Krawinkler H., 2000, Effects of near-fault ground motions on frame structures, *John A Blume Earthquake Engineering Center Report No. 138*, Dept. of Civil and Environmental Engineering, Stanford University, California.

Baez J.I., Miranda E., 2000, Amplification factors to estimate inelastic displacement demands for the design of structures in the near field, *Proceedings of the 12th World Conference on Earthquake Engineering*, New Zealand, No. 1561.

Bazzurro, P., 1998, Probabilistic seismic demand analysis, *Ph.D. Dissertation*, Department of Civil and Environmental Engineering, Stanford University, California (also available at http://pitch.stanford.edu/rmsweb/Thesis/PaoloBazzurro.pdf).

Bazzuro P., Cornell C.A., 1999, Disaggregation of seismic hazard, *Bulletin of the Seismological Society of America*, **89(2)**, 501-520.

Benjamin J.R., Cornell C.A., 1970, *Probability, Statistics, and Decision for Civil Engineers*, 1st edn, McGraw Hill, New York, 379,418.

Bozorgnia Y., Mahin S.A., 1998, Ductility and strength demands of near-fault ground motions of the Nortridge earthquake, *Proceedings of the 6th U.S. National Conference on Earthquake Engineering*, Seattle, Washington.

Chopra A.K., 1995, *Dynamics of Structures: Theory and Applications to Earthquake Engineering*, 1st edn, Prentice Hall, New Jersey, 444-447.

Collins K.R., Wen Y.K., Foutch D.A., 1995, Investigation of alternative seismic design procedures for standard buildings, *Civil Engineering Studies, Structural Research Series No. 600*, Dept. of Civil Engineering, University of Illinois at Urbana-Champaign.

Cordova P.P., Mehanny S.S.F., Deierlein G.G., Cornell C.A., 2001, Development of new seismic intensity measure and probabilistic design procedure, To be published in the *Proceedings of the 3rd U.S.-Japan Workshop on Performance-Based Seismic Design Methodology for Concrete Buildings*, Sapporo, Japan.

Cornell C.A., 1968, Engineering seismic risk analysis, *Bulletin of the Seismological Society of America*, **58(5)**, 1583-1606.

Cornell C.A., Luco N., 1999, The effects of connection fractures on steel moment resisting frame seismic demand and safety: A report on SAC Phase II Task 5.4.6, *Report No. SAC/BD-99/03*, SAC Joint Venture, Sacramento, California.

FEMA 273, 1997, *NEHRP guidelines for the seismic rehabilitation of buildings*, Building Seismic Safety Council, Washington, D.C.

FEMA 350-353, 2000, *Recommended seismic design criteria for new steel moment-frame buildings (350), Recommended seismic evaluation and upgrade criteria for existing welded steel moment-frame buildings (351), Recommended postearthquake evaluation and repair criteria for welded steel moment-frame buildings (352), and Recommended specifications and quality assurance guidelines for steel moment-frame construction for seismic applications (353)*, SAC Joint Venture, Sacramento, California.

Freeman S.A., Nicoletti J.P., Tyrell J.V., 1975, Evaluations of existing buildings for seismic risk – A case study of Puget Sound Naval Shipyard, Bremerton, Washington, *Proceedings of the 1st U.S. National Conference on Earthquake Engineering*, Berkeley, California, 113-122.

Gupta A., Krawinkler H., 1999, Seismic demands for performance evaluation of steel moment resisting frame structures, *John A. Blume Earthquake Engineering Center Report No. 132*, Dept. of Civil and Environmental Engineering, Stanford University, California.

Iwan W.D., 1980, Estimating inelastic response spectra from elastic spectra, *Earthquake Engineering and Structural Dynamics*, **8**, 375-388.

Liu J., Astaneh-Asl A., 2000, Cyclic testing of simple connections including effects of slab, *ASCE Journal of Structural Engineering*, **126(1)**, 32-39.

Luco N., 2001, Probabilistic seismic demand analysis, SMRF connection fractures, and near-source effects, *Ph.D. Dissertation*, Dept. of Civil and Environmental Engineering, Stanford University, California.

Mehanny, S.S.F., 1999, Modeling and assessment of seismic performance of composite frames with reinforced concrete columns and steel beams, *Ph.D. Dissertation*, Dept. of Civil and Environmental Engineering, Stanford University, California.

Prakash V., Powell G.H., Campbell S., 1993, DRAIN-2DX: Base program description and user guide, version 1.10, *Report No. UCB/SEMM-93/17*, Dept. of Civil Engineering, University of California at Berkeley.

SEAOC Blue Book, 1999, *Recommended lateral force requirements and commentary*, 7th edn, Structural Engineers Association of California, Sacramento, California.

Sewell R.T., 1989, Damage effectiveness of earthquake ground motion: Characterizations based on the performance of structures and equipment, *Ph.D. Dissertation*, Dept. of Civil and Environmental Engineering, Stanford University, California.

Shome N., Cornell C.A., Bazzurro, P., Carballo J.E., 1998, Earthquakes, records, and nonlinear responses, *Earthquake Spectra*, **14(3)**, 469-500.

Shome N., Cornell C.A., 1999, Probabilistic seismic demand analysis of nonlinear structures, *Reliability of Marine Structures Program Report No. RMS-35*, Department of Civil and Environmental Engineering, Stanford University, California (also available at http://pitch.stanford.edu/rmsweb/Thesis/NileshShome.pdf).

Somerville P.G., Smith N.F., Graves R.W., Abrahamson N.A., 1997a, Modification of empirical strong ground motion attenuation relations to include the amplitude and duration effect of rupture directivity, *Seismological Research Letters*, **68(1)**, 199-222.

Somerville P.G., Smith N., Punyamurthula S., Sun J., 1997b, Development of ground motion time histories for phase 2 of the FEMA/SAC steel project, *Report No. SAC/BD-97/04*, SAC Joint Venture, Sacramento, California.

Somerville P.G., 1998, Development of an improved ground motion representation for near fault ground motions, *SMIP98 Seminar on Utilization of Strong-Motion Data*, Oakland, California.

Song J., Ellingwood B.R., 1999, Seismic reliability of special moment steel frames with welded connections, II, *ASCE Journal of Structural Engineering*, **125(4)**, 372-384.

Veletsos A.S., Newmark N.M., 1960, Effect of inelastic behavior on the response of simple systems to earthquake motions, *Proceedings of the 2nd World Conference on Earthquake Engineering*, Tokyo, Japan, 895-912.

Younan A., Banon H., Marshall P., Crouse C.B., Cornell C.A., An overview of the ISO Seismic Guidelines, To appear in *Proceedings of the Offshore Technology Conference 2001*, Houston, Texas.